

**Zeitschrift:** Eclogae Geologicae Helvetiae  
**Herausgeber:** Schweizerische Geologische Gesellschaft  
**Band:** 89 (1996)  
**Heft:** 2

**Artikel:** Magnetostratigraphic calibration of the Oligocene to Middle Miocene (30-15 Ma) mammal biozones and depositional sequences of the Swiss Molasse Basin  
**Autor:** Schlunegger, Fritz / Burbank, Douglas W. / Matter, Albert  
**DOI:** <https://doi.org/10.5169/seals-167923>

### **Nutzungsbedingungen**

Die ETH-Bibliothek ist die Anbieterin der digitalisierten Zeitschriften. Sie besitzt keine Urheberrechte an den Zeitschriften und ist nicht verantwortlich für deren Inhalte. Die Rechte liegen in der Regel bei den Herausgebern beziehungsweise den externen Rechteinhabern. [Siehe Rechtliche Hinweise.](#)

### **Conditions d'utilisation**

L'ETH Library est le fournisseur des revues numérisées. Elle ne détient aucun droit d'auteur sur les revues et n'est pas responsable de leur contenu. En règle générale, les droits sont détenus par les éditeurs ou les détenteurs de droits externes. [Voir Informations légales.](#)

### **Terms of use**

The ETH Library is the provider of the digitised journals. It does not own any copyrights to the journals and is not responsible for their content. The rights usually lie with the publishers or the external rights holders. [See Legal notice.](#)

**Download PDF:** 01.04.2025

**ETH-Bibliothek Zürich, E-Periodica, <https://www.e-periodica.ch>**

# Magnetostratigraphic calibration of the Oligocene to Middle Miocene (30–15 Ma) mammal biozones and depositional sequences of the Swiss Molasse Basin

FRITZ SCHLUNEGGER<sup>1</sup>, DOUGLAS W. BURBANK<sup>2</sup>, ALBERT MATTER<sup>1</sup>,  
BURKHART ENGESSER<sup>3</sup> & CLEMENS MÖDDEN<sup>3</sup>

*Key words:* Magnetostratigraphy, Molasse Basin, biostratigraphy, foreland basins, mammalia

## ABSTRACT

Across the broad spatial and temporal expanse of the Alpine foreland basin, reconstruction of the relationships between basin subsidence, facies distribution and unroofing history of the Alpine wedge has been thwarted by the absence of a detailed chronologic framework. High resolution magnetostratigraphies, established on eight fossiliferous sections in the Lake Thun, Napf and Lake Zürich areas as well as in the Jura Mountains, provide the most complete temporal calibration of the Late Oligocene to Middle Miocene (30–15 Ma) mammal biozonation. The average duration of the 22 assemblage zones calibrated in this paper varies from 300 kyr in the Late Chattian to approximately 800 kyr in the Aquitanian to Langhian and in the Early Chattian. Furthermore the magnetic chronology suggests that the Paleogene/Neogene boundary should be placed within the mammal assemblage zone of Brochene Fluh 53.

The presented magnetostratigraphies greatly improve the temporal calibration of the depositional sequences in the North Alpine foreland basin between 30–15 Ma. The Lower Marine Molasse (UMM) regression in central Switzerland is dated with 30 Ma, which coincides with an eustatic sea level fall. The Upper Marine Molasse (OMM) transgression is strongly heterochronous and is calibrated with 21 Ma in Haute Savoie and 20 Ma in the Napf area, suggesting that the perialpine sea way expanded from west to east. The transition from marine OMM to continental Upper Freshwater Molasse (OSM) is time transgressive as well. In the center of the Napf fan, OSM conglomerates rest directly on Lower Freshwater Molasse (USM) with no OMM in between. 10 kilometers farther east the OMM regression is calibrated with 18.7 Ma as compared to 17 Ma in the interfan areas.

## ZUSAMMENFASSUNG

Die stratigraphische und strukturelle Entwicklung des Schweizerischen Molassebeckens ist in grossen Zügen bekannt. Mangelnde chronologische Daten aus dem nordalpinen Vorlandbecken bildeten das bedeutendste Hindernis, die kausale Beziehung zwischen Orogenese und den Prozessen im Vorlandbecken herzustellen.

Magnetostratigraphische Analysen acht fossilreicher Profile im Thunersee-, Zürichsee- und Napf-Gebiet sowie im Juragebirge bilden den umfassendsten chronologischen Rahmen des Schweizerischen Molassebeckens

---

<sup>1</sup> Geologisches Institut, Universität Bern, Baltzerstrasse 1, CH-3012 Bern

<sup>2</sup> Department of Geological Sciences, University of Southern California, Los Angeles, CA 90089-0740, USA

<sup>3</sup> Naturhistorisches Museum Basel, Geologische Abteilung, Augustinerstrasse 2, CH-4051 Basel

im Zeitabschnitt zwischen 30–15 Ma. 22 Säugetierzonen zwischen Frühem Chattian und Langhian werden zeitlich kalibriert. Dabei umfassen die Säugetierzonen einen Zeitbereich von 300 kyr im Späten Chattian und etwa 800 kyr im Frühen Chattian sowie im Zeitabschnitt zwischen Aquitanian und Langhian. Nach dieser neuen magnetostratigraphischen Chronologie wird die Paläogen/Neogen-Grenze in die Molasse-Säugetierzone von Brochene Fluh 53 gelegt.

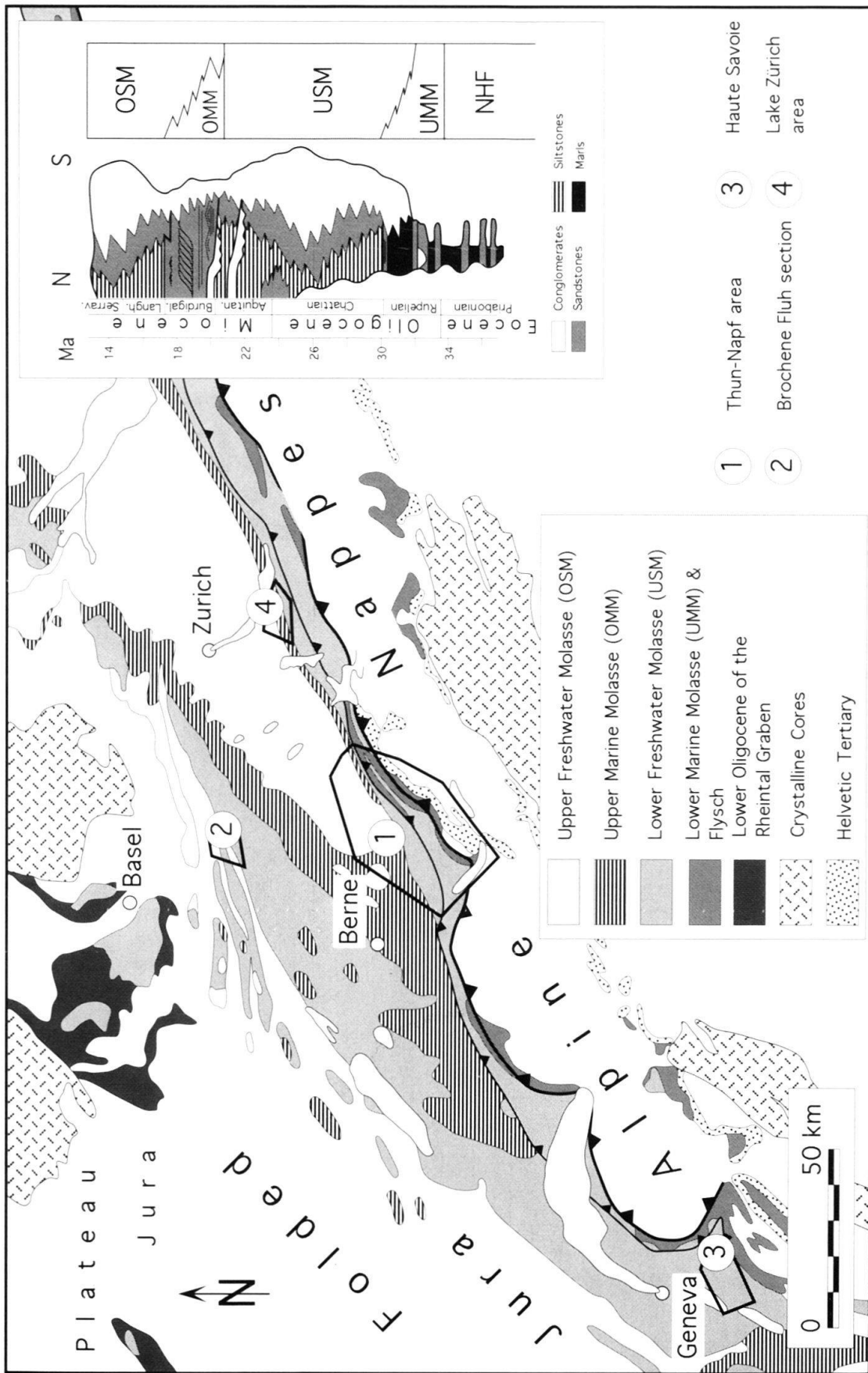
Die neue magnetostratigraphische Chronologie verbessert wesentlich die zeitliche Erfassung der Molassesequenzen. Die Regression der Unteren Meeremolasse (UMM) wird in der Zentralschweiz mit 30 Ma datiert und fällt zeitlich mit einer globalen Meeresspiegelabsenkung zusammen. Die Transgression der Oberen Meeremolasse (OMM) erweist sich als heterochron und erfolgte in Haute Savoie um 21 Ma und im Napfgebiet um 20 Ma. Dabei werden frühere Vermutungen bestätigt, dass sich das perialpine Meer von Westen gegen Osten ausdehnte. Die Regression der OMM ist ebenfalls heterochron. Im Zentrum des Napfschuttfächers wird die OMM von kontinentaler Oberer Süßwassermolasse (OSM) ersetzt, so dass OSM Konglomerate direkt auf Unterer Süßwassermolasse (USM) liegen. 10 Kilometer weiter östlich wird die OMM Regression mit 18.7 Ma datiert, und in Bereichen zwischen Schuttfächern erfolgte sie bei 17 Ma.

## Introduction

The Molasse Basin, on the northern side of the Alps (Fig. 1), is a classical foreland basin of Oligocene and Miocene age. The depositional history of this basin, with its deep-water (flysch) phase followed by continental and shallow-water (molasse) deposits is largely controlled by the evolution of the Alpine orogenic wedge. Therefore, the development of the Molasse Basin has attracted structural geologists (Pfiffner 1986; Burkhard 1990) as well as sedimentologists (e.g. Diem 1986; Keller 1989) and basin modellers (Homewood et al. 1986; Sinclair et al. 1991; Sinclair & Allen 1992). These studies focussed on facies distribution and relationships between the evolution of the orogenic wedge and the stratigraphic, sedimentological and structural response in the basin. As pointed out by Burbank et al. (1992), however, time control within the foreland is crucial for understanding the causal relationships between basin subsidence, facies distribution and unroofing history of the Alpine wedge. Although a detailed mammal biozonation based on faunas from more than 100 localities has been established by Engesser & Mayo (1987), the faunal data do not allow precise correlation of sedimentary processes in the Molasse Basin with the cooling history of the Alpine hinterland (see also Schlunegger et al. 1993).

Five lithostratigraphic units are distinguished in the Molasse-Basin, for which the German abbreviations are used for convenience (Matter et al. 1980; Keller 1989; Sinclair et al. 1991; Fig. 1): North Helvetic Flysch (NHF), Lower Marine Molasse (UMM), Lower Freshwater Molasse (USM), Upper Marine Molasse (OMM) and Upper Freshwater Molasse (OSM). The Molasse deposits form two coarsening- and shallowing-upward megasequences. The first megasequence begins either with Lutetian to Priabonian NHF or with the Rupelian UMM, which are followed by the Chattian and Aquitanian fluvial clastics of the USM. The second megasequence, starting with the Burdigalian transgression, consists of shallow marine sandstones (OMM), which interfinger with major fan deltas adjacent to the thrust front (Berli 1985; Keller 1989; Hurni 1991; Schlunegger et al. 1993). This megasequence ends with Serravalian fluvial clastics of the OSM.

A first attempt to improve the chronologic framework in the Alpine foreland with magnetostratigraphy was successfully carried out by Burbank et al. (1992) for the late Chattian and Aquitanian fossiliferous strata in the western Molasse. Given this initial



Modified after Keller et al. (1990)

Fig. 1. Geological map of the Swiss Molasse Basin.

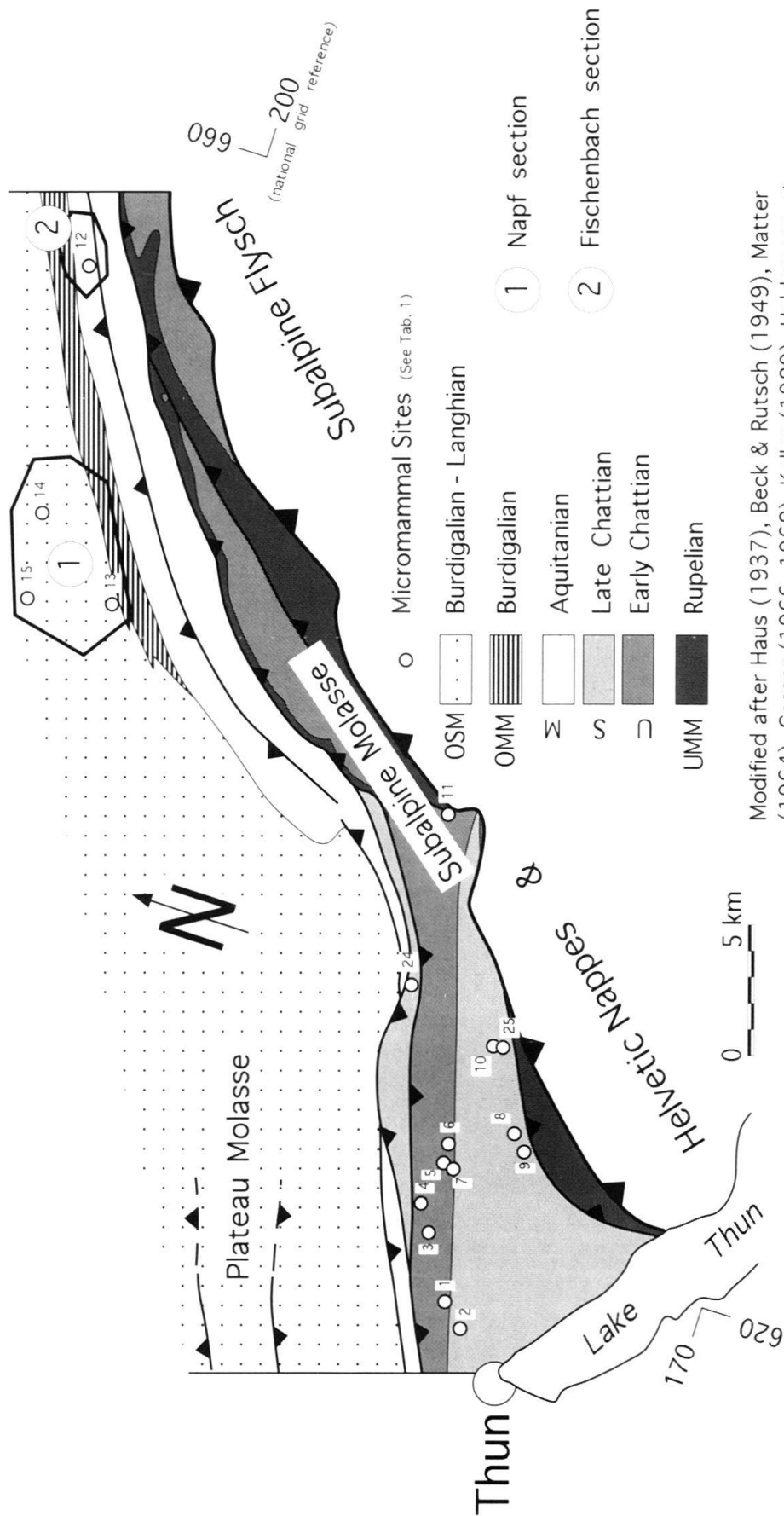
success, an effort to calibrate the entire stratigraphic range of the Molasse was undertaken. Magnetic polarity stratigraphies, ranging in age from Rupelian to Langhian, were established on eight fossiliferous sections in central Switzerland, the Lake Zürich area and the Jura Mountains (Fig. 1). The main aim of this paper is to present these magnetostratigraphic results and thereby establish a chronologic control on the faunal and depositional record. This, in turn, will provide a temporal calibration for the facies relationships and for the response of the basin to Alpine tectonic events as well as for the denudation history of the evolving orogen. The magnetostratigraphies will also give chronologic constraints for the continental paleoclimatic record of the Molasse.

### Geological setting

The study areas lie at the Subalpine thrust front, where deep river cuts provide good exposures in the otherwise densely vegetated cover of the foreland and in the Jura Mountains (Fig. 1). The Napf-Thun area, located at the proximal basin margin, is composed of southeast-dipping thrust sheets of the Subalpine Molasse and the generally flat-lying southernmost Plateau Molasse, thus encompassing the entire Molasse sequence from UMM to OSM (Fig. 2). Rupelian to Aquitanian fossiliferous sequences are exposed in the Subalpine Molasse of the Thun area, whereas Aquitanian to Langhian strata crop out in the Plateau Molasse of the Napf area. The Sihl section southwest of Lake Zürich (Fig. 1) is situated in the upturned Plateau Molasse and consists of Aquitanian USM. The section located within the Jura Mountains represents the distal facies deposited at the feather-edge of the basin. It is made up of a succession of lacustrine carbonates of uppermost Chattian age (Baumberger 1927; Engesser 1990).

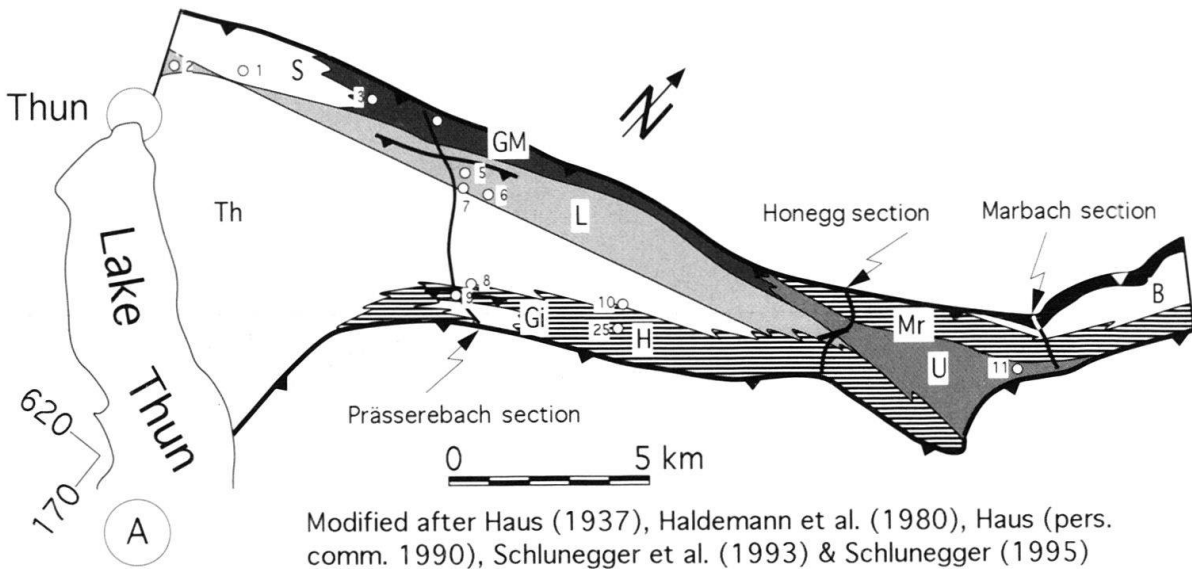
Previous studies of the Subalpine Molasse thrust sheets northeast of Lake Thun, combined with further detailed mapping, provide a lithostratigraphic framework and an initial temporal scheme that indicate strong heterochronous facies relationships (Fig. 3). This area was chosen for magnetostratigraphic calibration of the late Rupelian to earliest Aquitanian mammal assemblage zones because of the presence of three thick representative sections (Prässerebach, Honegg, Marbach) calibrated by numerous fossil sites (Haus 1937; Engesser 1990; Schlunegger et al. 1993). Moreover, detailed sedimentological studies as well as mapping reveal a continuous stratigraphic record for these sections except for a hiatus at the base of the Prässerebach section (Haus 1937; Diem 1986; Schlunegger et al. 1993; Schlunegger 1995).

Chronological studies on Aquitanian to Langhian clastic deposits have been carried out in the Napf area (Fig. 2). The region including and surrounding the Napf fan has been the focus of many previous stratigraphic studies, which yielded abundant biostratigraphic, lithostratigraphic and tectonic data (Matter 1964; Gasser 1966; Keller 1989; Engesser 1990; Hurni 1991). Two new magnetostratigraphic sections (Napf and Fischenbach, Fig. 2) in the north-dipping Plateau Molasse serve to document the Aquitanian (Fischenbach section), as well as the late Burdigalian to Langhian chronology (Napf sections, Fig. 4). In this area, major erosional unconformities were identified both within the USM as well as between USM and OMM on a seismic line across central Switzerland (Fig. 4; Schlunegger 1995). A further section through the upper USM was measured along the Sihl river in the Lake Zürich area (Fig. 1) in an effort to cover more completely the numerous reversals in the Aquitanian.



Modified after Haus (1937), Beck & Rutsch (1949), Matter (1964), Gasser (1966, 1968), Keller (1989), Haldemann et al. (1980), Schlunegger et al. (1993) & Schlunegger (1995)

Fig. 2. Geological map of the Thun-Napf area.



Facies

- Conglomerates
- Cgl. & Sandstones
- Cgl., Sand- & Siltstones
- Sand- & Siltstones
- Silt- & Mudstones
- Marine (UMM)



Mammal Sites (See Tab. 1)

- B: Beichlen Formation
- Mr: Molasse rouge Formation
- U: Uerscheli Formation
- GM: Granitic Molasse Formation
- S: Schwändibach Conglomerate
- L: Losenegg Formation
- Th: Thun Formation
- H: Honegg Marls Formation
- Gi: Gitzischöpf Conglomerate

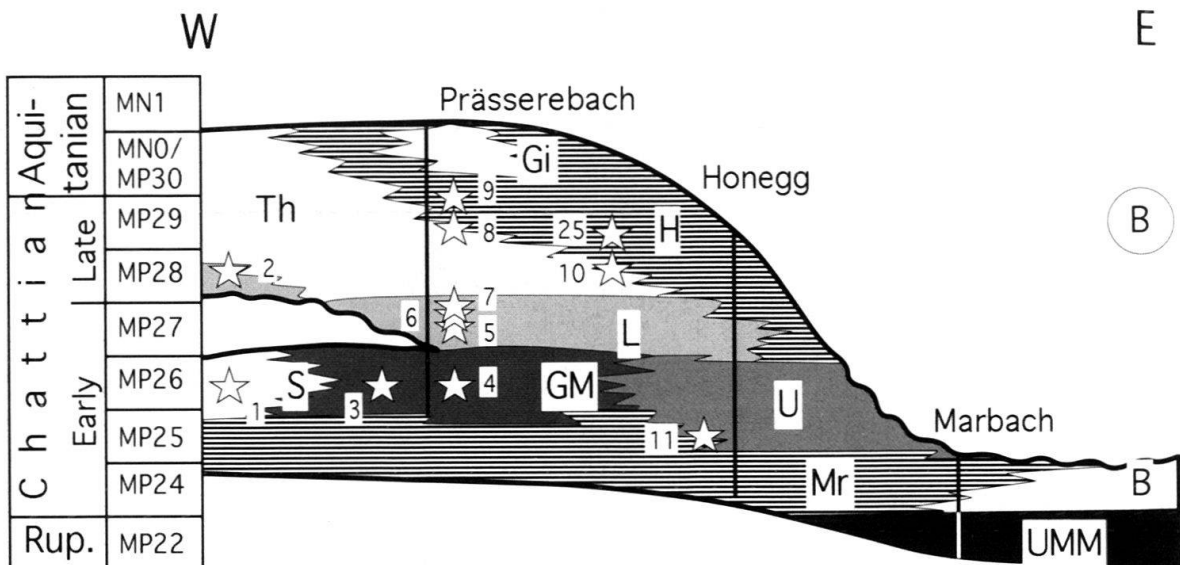


Fig. 3. Stratigraphy of the Subalpine Molasse northeast of Thun with a) geological map, showing locations of analyzed sections and b) chronologic (Wheeler) diagram.

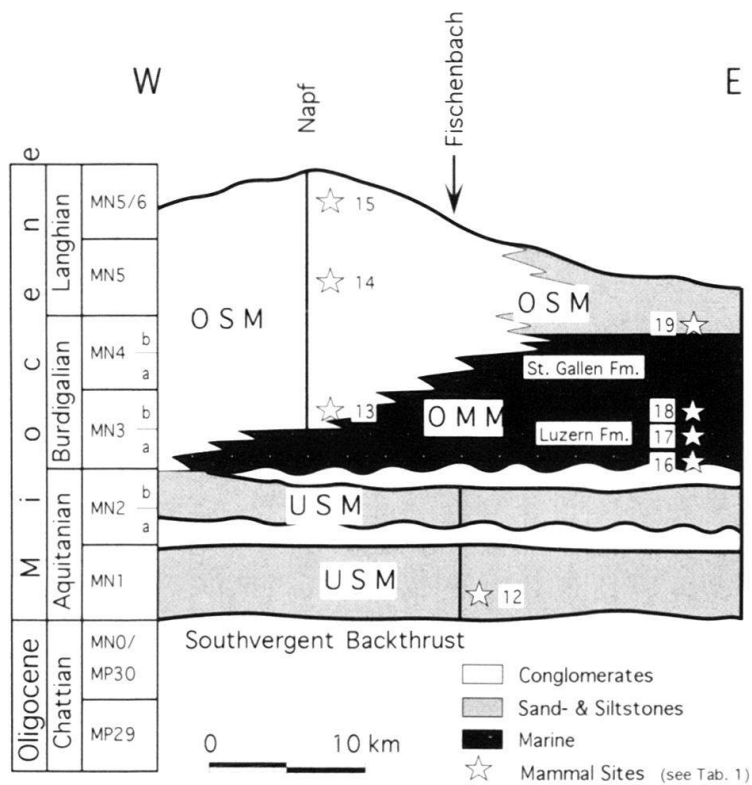


Fig. 4. Chronologic (Wheeler) diagram of the Plateau Molasse of the Napf area.

The 70-m-thick Brochene Fluh section in the Jura Mountains includes all three mammal assemblage zones between MP29 and MP30, suggesting continuous sedimentation (Baumberger 1927; Engesser 1990). This section provides additional detailed magnetostratigraphic constraints on the geochronology of the uppermost Chattian.

Finally, the magnetostratigraphic results, which were gained on two sections in Haute Savoie (Fig. 1, Burbank et al. 1992), are incorporated into this study as they provide good chronologies for the Late Chattian to Aquitanian. However, the magnetostratigraphies of both sections are herein recalibrated because they were originally correlated with the magnetic polarity time scale (MPTS) of Berggren et al. (1985), which has since been superseded by the revised version of the MPTS of Cande & Kent (1992, 1995).

## Methods

### *Lithostratigraphy and mammal paleontology*

Formal and informal lithostratigraphic units were defined and mapped in the proximal Molasse of the study area. In total, 10 sections, of which 8 are used in this paper, were carefully measured. For a full account of the lithostratigraphy and sedimentology of the USM between Berne and Zürich, the reader is referred to Schlunegger (1995).

A biostratigraphic data base of micromammals from the proximal Molasse of central Switzerland and the Brochene Fluh section in the Jura mountains (Fig. 1) was compiled from the literature (Tab. 1). To improve the biostratigraphic control, additional dark



Tab. 1. Mammal sites of the study area.

Site No.	Site Name	Assemblage Zone	MP/MN Zone	Reference/ National Grid	New Fauna
1	Schwändlbach	Oensingen	MP26	Engesser (1990)	
2	Schwandenbad	Formant 6 - Br. Fluh 53	MP28 - MP30	615900 179675	Adelomyarion sp., Eomyodon cf. volkeri, Insectivor indet. Suide indet.
3	Trimmlen	Oensingen	MP26	619250 181500	Archaeomys gervaisi
4	Loch	Oensingen	MP26	620725 182100	Archaeomys gervaisi
5	Losenegg 3	Wynau 1	MP27	622375 181500	Archaeomys robustus
6	Losenegg 2	Boningen	MP27	Engesser (1990)	
7	Cheistlisteg	Wynau 1 - Formant 6	MP27 - MP28	622425 181125	Eomys ebnatensis
8	Dürenschwand	Formant 6	MP28	624100 179200	Eomys major
9	Prässerebach	Rickenbach - Bourdry 2	MP29 - MN1	Engesser (1990)	
10	SEB6	Formant 6	MP28	128050 181250	Issidoromys limognensis
11	Bumbach 1	Bumbach 1	MP25	Engesser (1990)	
12	Fisch 2	Formant 11 - La Chau	MN1 - MN2a	153500 205325	Ritteneria or Rhodanomys schlosseri
13	Hasenbach 1	Hintersteinbruch	MN3b	Engesser (1990)	
14	Eimättli	Vermes 1	MN5	Matter (1964), Hurni (1991)	
15	Oeschgraben	Rümlikon	MN5/6	Matter (1964), Hurni (1991)	
16	Lc 1b/18		MN3a or younger	Keller (1989)	
17	Lu 10/76		MN3a or younger	Keller (1989)	
18	Hi 2/6		MN3b	Keller (1989)	
19	Halten		MN4	Keller (1989)	
20	Br. Fluh 4/5	Rickenbach+	MP29	Engesser (1990)	
21	Br. Fluh 19/20	Küttigen-	MP30	Engesser (1990)	
22	Br. Fluh 32	Küttigen	MP30	Engesser (1990)	
23	Br. Fluh 53	Br. Fluh 53	MP30	Engesser (1990)	
24	Hombach 3	Formant 6	MP28	Engesser (1990)	
25	Eriz 4	Wynau 1 - Rickenbach	MP27-MP29	628050 181175	Plesiomithus sp., Eucricetodon sp., Eomys ebnatensis Archaeomys sp.

coloured siltstones and argillaceous mudstones, which are prone to contain mammalian remains, were sampled. The material was dried, disaggregated and washed through a 0.5 mm sieve. The residue was studied under a binocular microscope and the vertebrate fragments were hand-picked.

In this study, the regional mammal biozonation of Engesser & Mayo (1987) and Engesser (1990) is used. It was established in the western and central Molasse with modifications by Mödden & Gad (1992) and Mödden (1993). This biozonation consists of 22 assemblage zones in the studied interval and therefore has a much higher resolution than the European MP/MN zonations (Mediterranean Palaeogene and Neogene mammalian zonation; Schmidt-Kittler 1987; Mein 1975, 1989; Fahlbusch 1991). A temporal calibration of this zonation has already been established by several authors using radiometric and magnetostratigraphic techniques (Pavoni & Schindler 1981; Steininger et al. 1990; Burbank et al. 1992; Berger 1992; Bolliger 1992; Krijgsman et al. 1994; Agustí et al. 1994; Barberà et al. 1994; Steininger 1994). However, the MP and MN zonations which are valid for the whole of Europe have a major drawback: the reference faunas are scattered all over Europe which raises the risk of heterochronies (Berger 1990). Consequently, an MP/MN zone established, for example, in Spain, may have no species in common with a fauna from Central Europe, even though both are calibrated within the MP/MN scheme (Bolliger 1992; Krijgsman et al. 1994). Therefore we strictly use the Molasse mammal assemblage zonations and their correlation to the MP/MN scheme as given by Engesser (1990).

### *Magnetostratigraphy*

The biostratigraphic data suggest that the magnetic sections located in proximal versus distal parts of the Molasse Basin (Fig. 1) are characterized by strong contrasts in sediment-accumulation rates. Therefore, an individual sampling strategy had to be defined for each section dependent on the availability of mud- and siltstones, biostratigraphically defined timespan and the expected number of reversals. The sample density varied from 2 to 3 m in the distal sections with supposedly condensed sedimentation, to 20 to 50 m in the proximal Molasse. In the distal clastics of the Napf area, magnetic sites were collected every 5 to 10 m in an attempt to resolve the very short reversals within the Aquitanian. According to Talling & Burbank's criteria (1993), this sampling array should be sufficiently dense to permit correlation of the local magnetic polarity stratigraphy (MPS) with the global magnetic polarity time scale (MPTS).

In the sampled sections, brown laminated mudstones yielded the most stable magnetic vectors and appeared most suitable for paleomagnetic studies. Coarser siltstones and fine sandstones, however, were sampled where no mudstones were available. At least four oriented specimens were taken for each sample site. Occasionally the only fine-grained material present were organic-rich marine marls or lacustrine limestones. In analogous modern depositional environments it has been observed that production and especially destruction of magnetic minerals by microbacteria can lead to magnetically weak and unstable samples (Karlin & Lewi 1983; Karlin 1990; Hawthorne & McKenzie 1993). This typically occurs when hematite and magnetite are reduced to sulfide under anaerobic conditions. During thermal demagnetization studies, oxidation of these sulfides occurs at  $\sim 375^{\circ}\text{C}$ , as indicated by a sudden increase in magnetic susceptibility

(Bentham 1992). Above this temperature, derivation of a reliable magnetic direction is typically not possible during thermal demagnetization. However, using a combined method with thermal and alternating field demagnetization allows detection of magnetic fields of oxides and sulfides without creating new minerals (Bentham 1992). Hence, even in organic-rich marine marls and lacustrine carbonates of the Molasse stable magnetic directions could be defined based on at least five to six specimens per site.

Red clay- and siltstones usually carry a chemical remanent magnetization, which has strong magnetic intensities. However, this type of magnetization may be acquired over a long period of time during which the earth's magnetic field may vary, resulting in an unstable and ambiguous signal. Therefore, double the usual number of samples per site were taken in red bed facies to test magnetic stability and reliability of the sampled horizon.

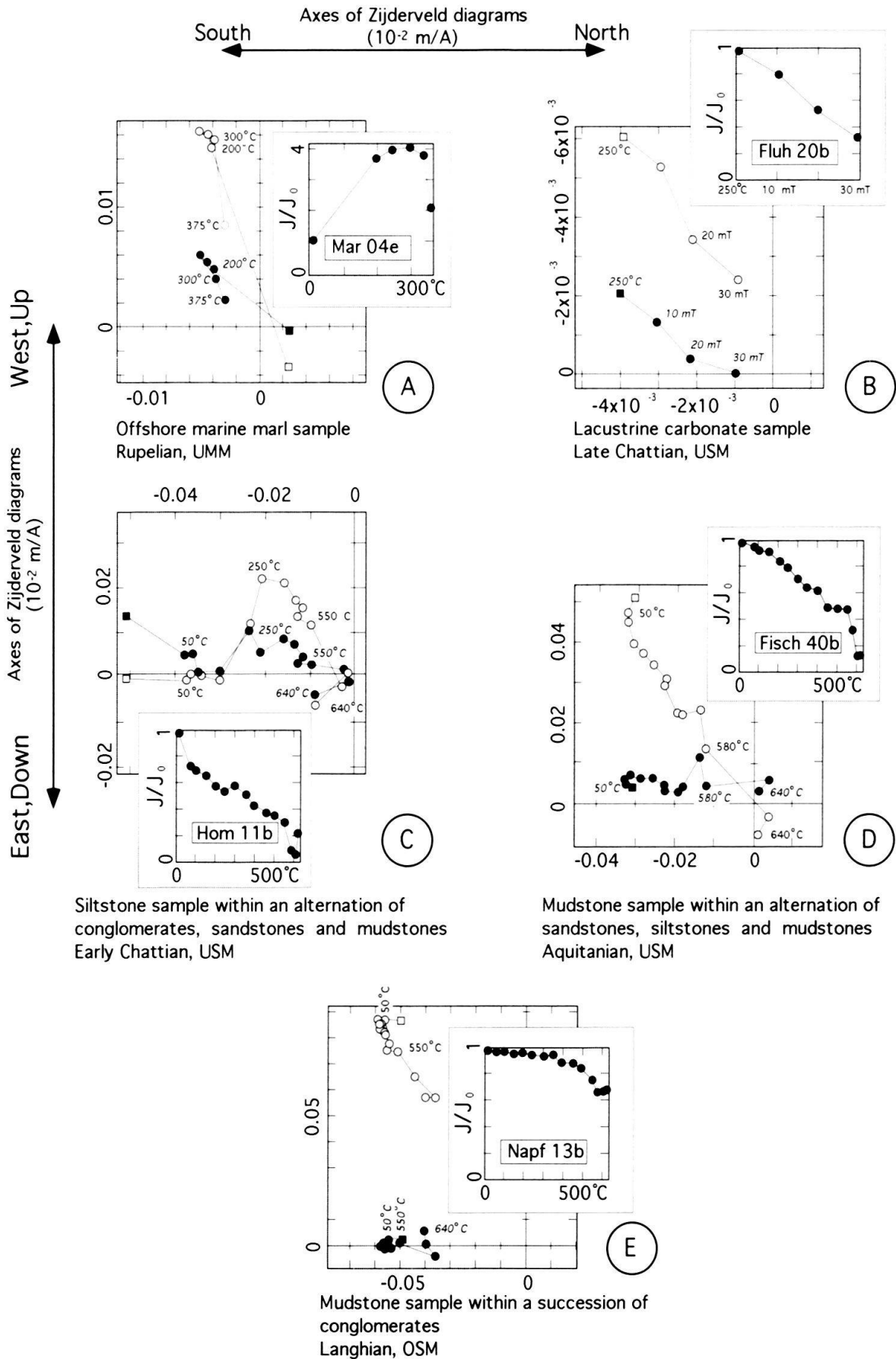
### Pilot studies

Ten pairs of specimens were chosen from each section as pilot specimens for demagnetization analysis. The criteria for selection were that (i) each lithology is represented, (ii) the pilot specimens cover the entire stratigraphic range of the section and (iii) each depositional system is represented by a pilot specimen. The pilot specimens were demagnetized in steps of 50°C from room temperature up to 550°C with a cryogenic magnetometer. Additionally, the temperature levels of 580°C, 610°C and 640°C were analyzed, after which some samples reached the noise level of the magnetometer ( $2\text{--}3 \times 10^{-5}$  A/m). After each step, the susceptibility of the pilot samples was measured to identify any change of magnetic minerals during sample processing.

Strikingly different behaviours emerged during this process between organic-rich samples (lacustrine carbonates and marine marls) and brown to reddish terrestrial samples. Reversed sites of lacustrine carbonates and marine marls (Fig. 5a) reveal that a normal component was removed between initial measurement (room temperature) and 250°C as suggested by the demagnetization vector on the demagnetization plot. Removal of this low temperature magnetic component, which is most probably carried by titanomagnetite (Butler 1992), is associated by an increase of the magnetic intensity from initially  $4 \times 10^{-5}$  A/m to  $20 \times 10^{-5}$  A/m (Fig. 5a). Between 250°C and 350°C a stable demagnetization path towards the origin is observed. At 400°C, however, striking increases in both magnetic susceptibilities (Fig. 6) and intensities accompanied by fluctuating magnetic directions indicate oxidation of sulfides to probably magnetite (Butler 1992). Therefore, organic-rich samples were tested using a mixed demagnetization method (Fig. 5b). First they were heated up to 250°C to remove the low-temperature overprint. Further demagnetization with alternating magnetic fields at 10-mT-steps revealed stable demagnetization paths towards the origin. Using this approach, organic-rich marine and lacustrine pilot specimens revealed a characteristic remanence direction at 250°C despite the somewhat variable behaviour during demagnetization.

---

Fig. 5. Demagnetization plots and intensity-loss ( $J/J_0$ ) plots for pilot specimens.



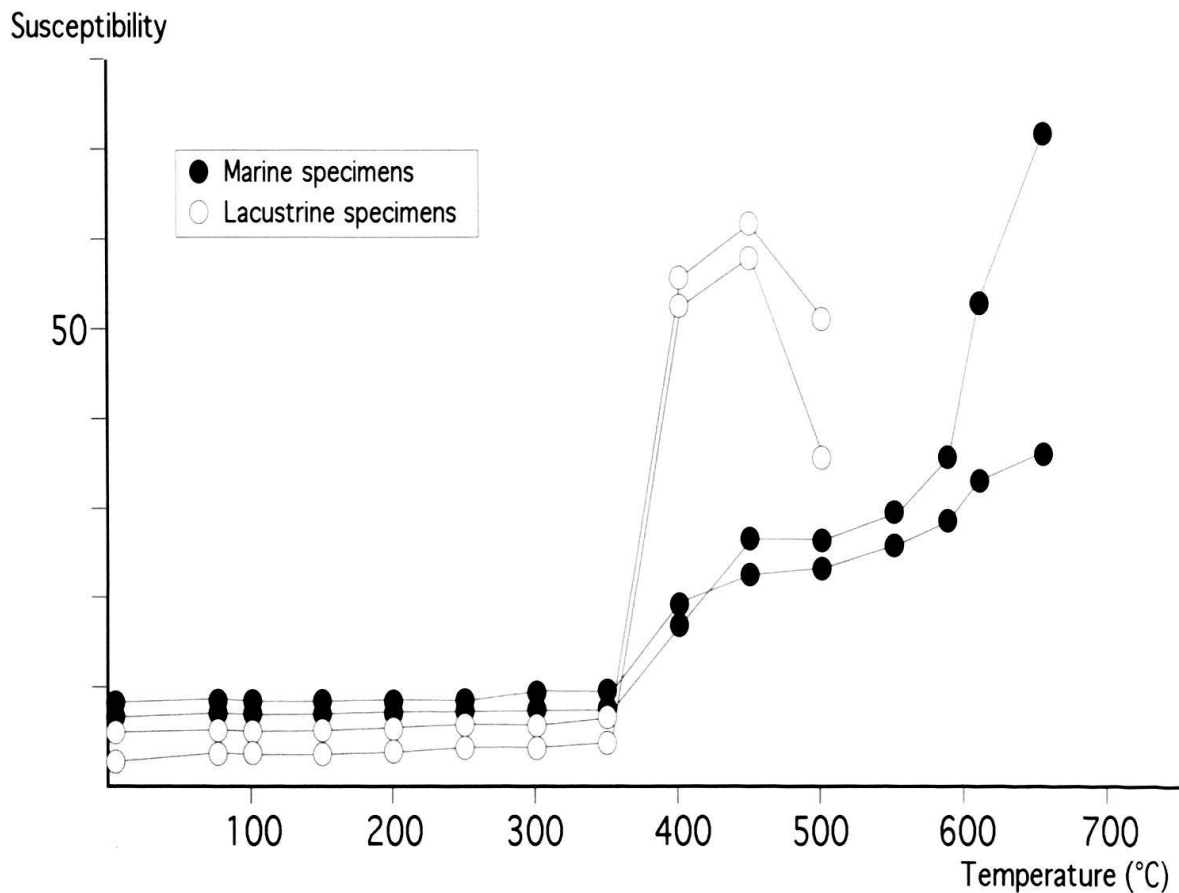


Fig. 6. Susceptibility versus temperature plot of organic-rich specimens.

Brown to reddish mudstones reveal highly varying initial magnetic intensities between  $50 \times 10^{-5}$  A/m to  $100 \times 10^{-5}$  A/m. They change their magnetic directions and loose magnetic intensities in the order of 20% between room temperature and  $250^{\circ}\text{C}$  as a low temperature overprint is removed (Fig. 5c). Further heating to  $550^{\circ}\text{C}$  removes at least 40% of the bulk intensity and reveals a stable demagnetization path towards the origin. Consequently the characteristic remanent magnetization of brown to reddish mudstone samples can be defined within a  $250^{\circ}$ – $550^{\circ}\text{C}$  temperature window (Fig. 5c–e). At  $580^{\circ}\text{C}$ , there is a major drop in magnetic intensity (20–50% of the bulk intensity) as the Curie temperature for magnetite is surpassed. At higher temperatures, these samples revealed different behaviours. Samples from the Aquitanian USM (Fig. 5d) reveal weak intensities at temperatures  $>600^{\circ}\text{C}$  and a high temperature overprint or a depositional remanence, both of which are most probably carried by hematite. However, magnetic intensities of Early Chattian specimens (Fig. 5c) increase at  $580^{\circ}\text{C}$  possibly due to oxidation of small magnetite grains during sample processing. Specimens from Burdigalian to Langhian deposits (Fig. 5e) loose little magnetic intensity at  $580^{\circ}\text{C}$ . The remaining field, which is most probably carried by hematite, reveals the same magnetic polarity, and no overprint is observed.

For all collected specimens the direction of the characteristic remanent magnetization can be defined at 250°C regardless of the somewhat variable behaviour during demagnetization, the apparent differences in intensities and variation in depositional systems. Based on the results of the pilot studies, the remaining samples were heated and measured at three heating steps between 250°C and 550°C for brown to reddish lithologies and between 250°C and 350°C for lacustrine and marine specimens. The coherence of the magnetic directions for each site was tested using Fisher (1953) statistics. Sites were classified as class I if three samples are grouped with  $k \geq 10$ . They were classified as class II if  $k < 10$  for three, but  $k \geq 10$  for two samples which yielded an unambiguous site polarity. Class III sites yielded no coherent directions and were not used to determine magnetic polarity. The mean magnetic vector of each class I and II site was used to calculate the virtual geomagnetic pole (VGP; McElhinny 1964, 1973). The latitude of the VGP formed the basis for the local MPS. Finally an  $\alpha_{95}$  error envelope was calculated for each VGP latitude.

### Reversal tests

Antipodal directions for all class I sites were plotted on a stereonet (Fig. 7) to test each section for antipolarity using the method by McElhinny (1964, 1973). The magnetic data from the Fischenbach, Prässerebach and Napf sections clearly pass the reversal test (Fig. 7a–c). The inclinations of the Fischenbach data are shallower than expected, however, which is probably due to compaction of the fine grained floodplain deposits during tectonic deformation and rotation of the beds to a vertical position (see also Brennan, 1993). Samples from the upper part of the Prässerebach section (Gitzschöpf Cgl., Fig. 3) were excluded from the reversal test as this unit reveals strong bedding-parallel rotation due to tectonic deformation.

The samples of the Honegg, Marbach and Brochene Fluh sections (Fig. 7d–f) fail the reversal test either because of too few samples (Fig. 7d) or because of post-depositional growth of minerals with a high Curie temperature such as hematite (Fig. 7e & f). However, as shown by the pilot specimens (Fig. 5), the intensities of these secondary mineral phases are too weak to have a significant influence on the characteristic remanent magnetization. No fold test can be applied to the sections as they are all uniformly dipping.

## Results

### *Thun area (Rupelian – earliest Aquitanian)*

Three sections (Marbach, Honegg, Prässerebach) form a composite sequence from Rupelian to Aquitanian (Fig. 3) with a large variety of facies, from offshore marine marls to alluvial fan conglomerates.

The Marbach section (Fig. 8) consists of 75 m of Rupelian marls and sandstones (UMM), overlain by 785 m of USM. The USM comprises three lithostratigraphic units: alternations of conglomerates and mudstones (Beichlen Formation), sandstones and mudstones (Molasse rouge Formation) and sandstones and siltstones (Uerscheli Sandstone).

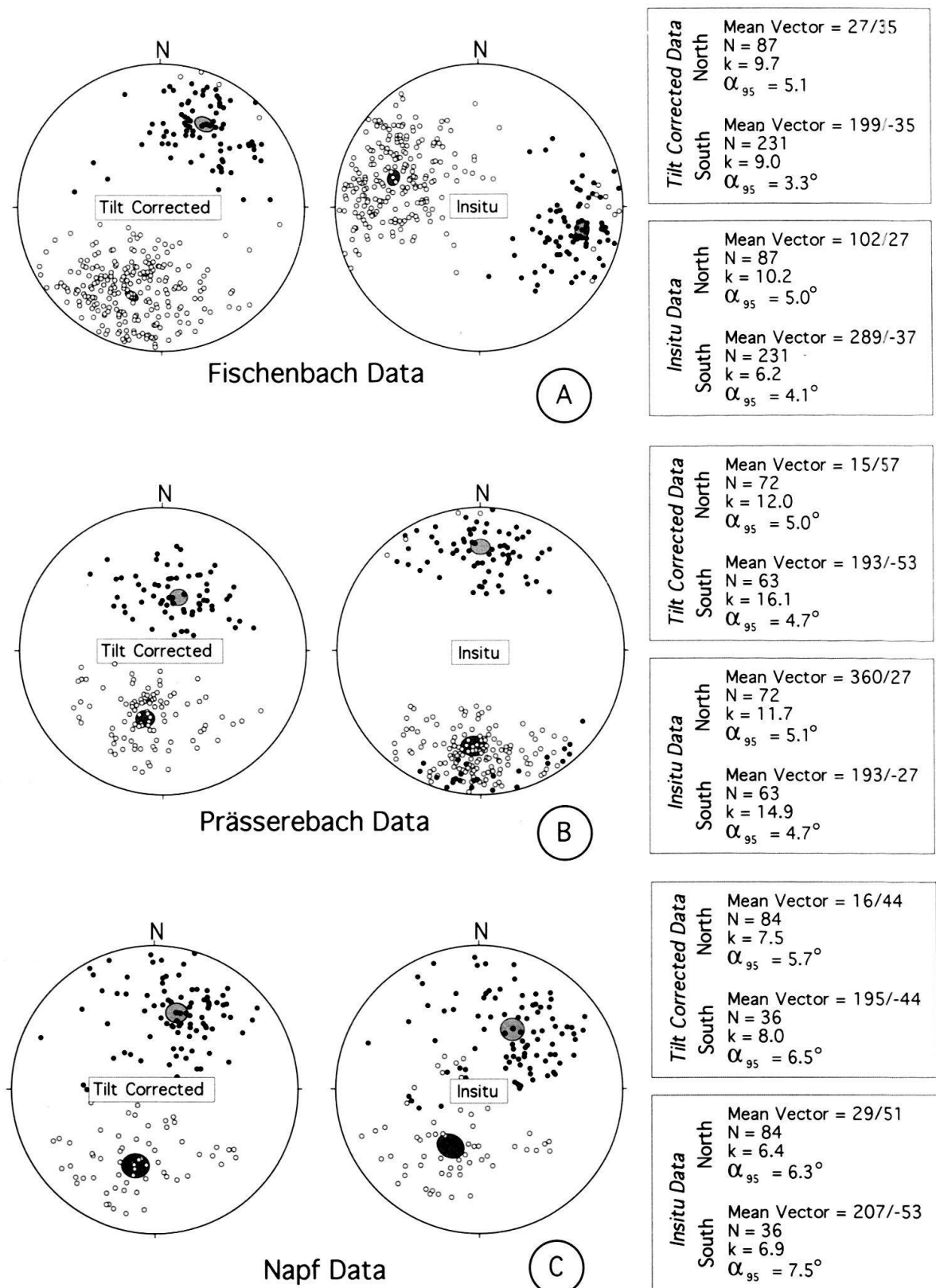
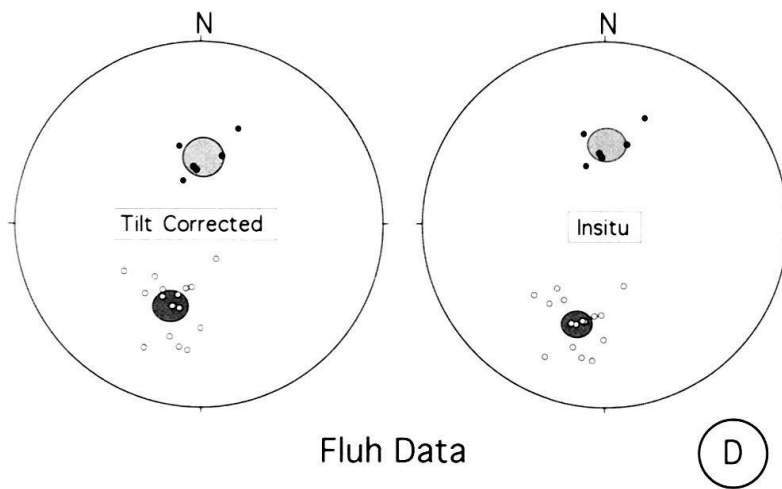
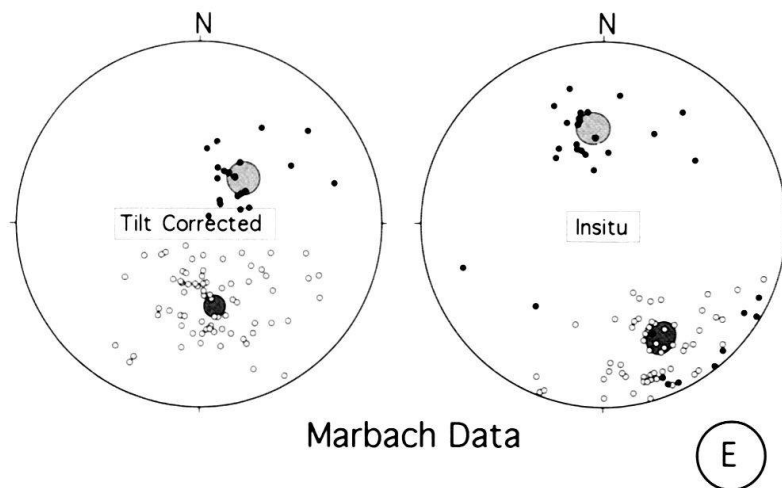


Fig. 7. Stereonet plot of class I normally (filled circles, lower hemisphere) and reversely (open circles, upper hemisphere) magnetized data.



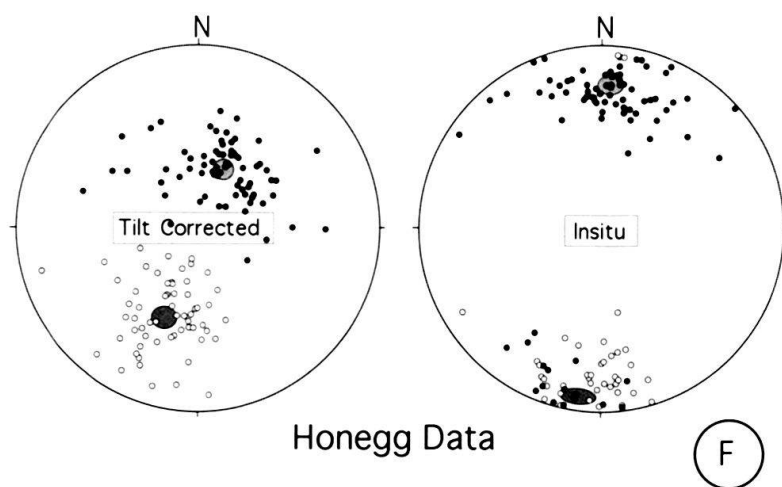
<i>Tilt Corrected Data</i>	North	Mean Vector = 1/60 N = 6 k = 43.7 $\alpha_{95} = 8.9^\circ$
	South	Mean Vector = 199/-50 N = 15 k = 23.9 $\alpha_{95} = 7.6^\circ$

<i>In situ Data</i>	North	Mean Vector = 3/54 N = 6 k = 44.6 $\alpha_{95} = 8.7^\circ$
	South	Mean Vector = 196/-42 N = 15 k = 28.3 $\alpha_{95} = 6.9^\circ$



<i>Tilt Corrected Data</i>	North	Mean Vector = 43/62 N = 21 k = 18.8 $\alpha_{95} = 7.3^\circ$
	South	Mean Vector = 171/-53 N = 69 k = 11.3 $\alpha_{95} = 5.2^\circ$

<i>In situ Data</i>	North	Mean Vector = 354/46 N = 21 k = 18.2 $\alpha_{95} = 7.4^\circ$
	South	Mean Vector = 160/-31 N = 69 k = 11.9 $\alpha_{95} = 5.1^\circ$



<i>Tilt Corrected Data</i>	North	Mean Vector = 23/61 N = 72 k = 13.0 $\alpha_{95} = 4.8^\circ$
	South	Mean Vector = 201/-47 N = 60 k = 14.0 $\alpha_{95} = 5.0^\circ$

<i>In situ Data</i>	North	Mean Vector = 3/22 N = 72 k = 14.3 $\alpha_{95} = 4.5^\circ$
	South	Mean Vector = 188/-5 N = 60 k = 13.2 $\alpha_{95} = 5.2^\circ$



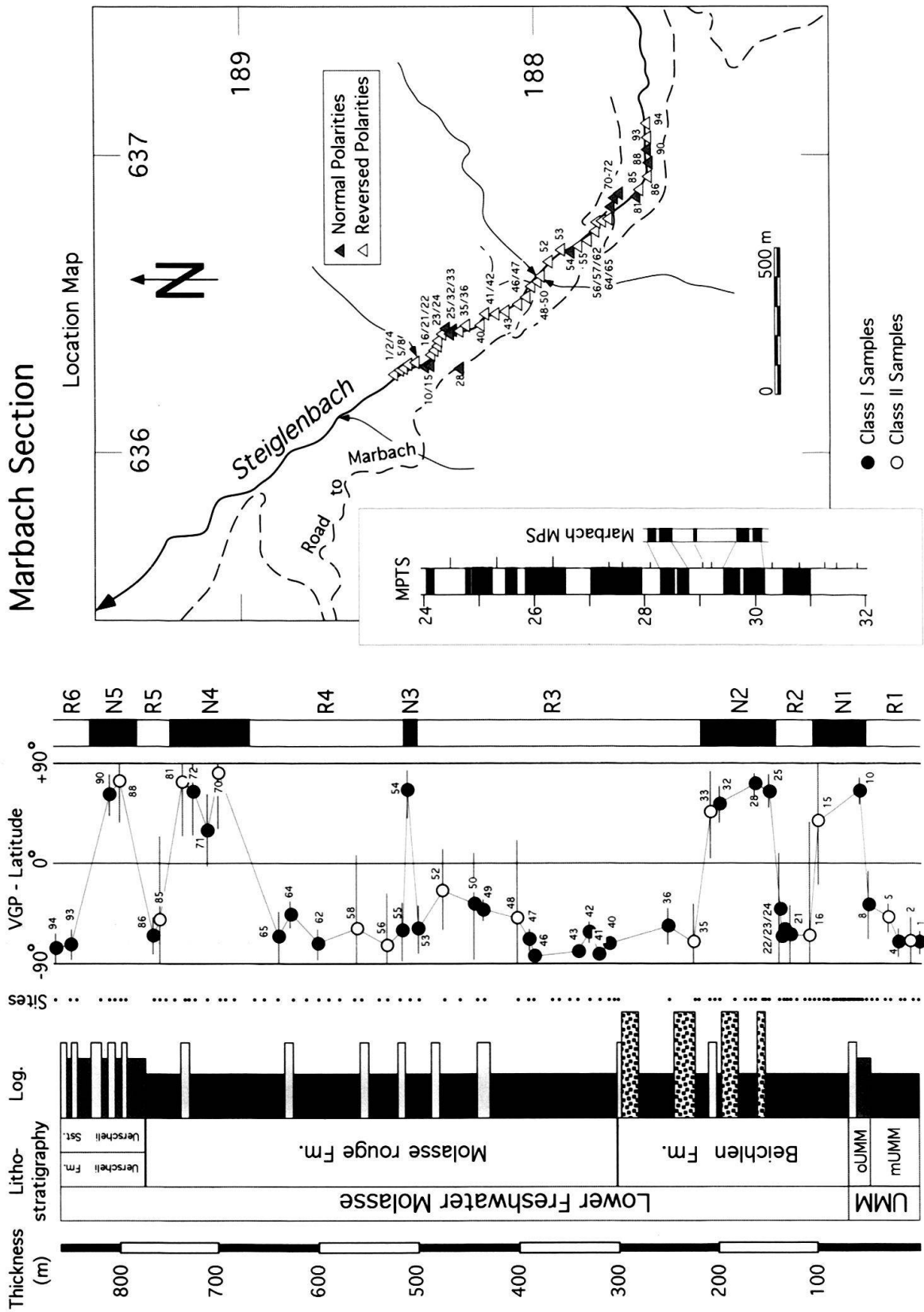


Fig. 8. Magnetostratigraphy of the Marbach section. For legend see Fig. 13.

Honegg Section

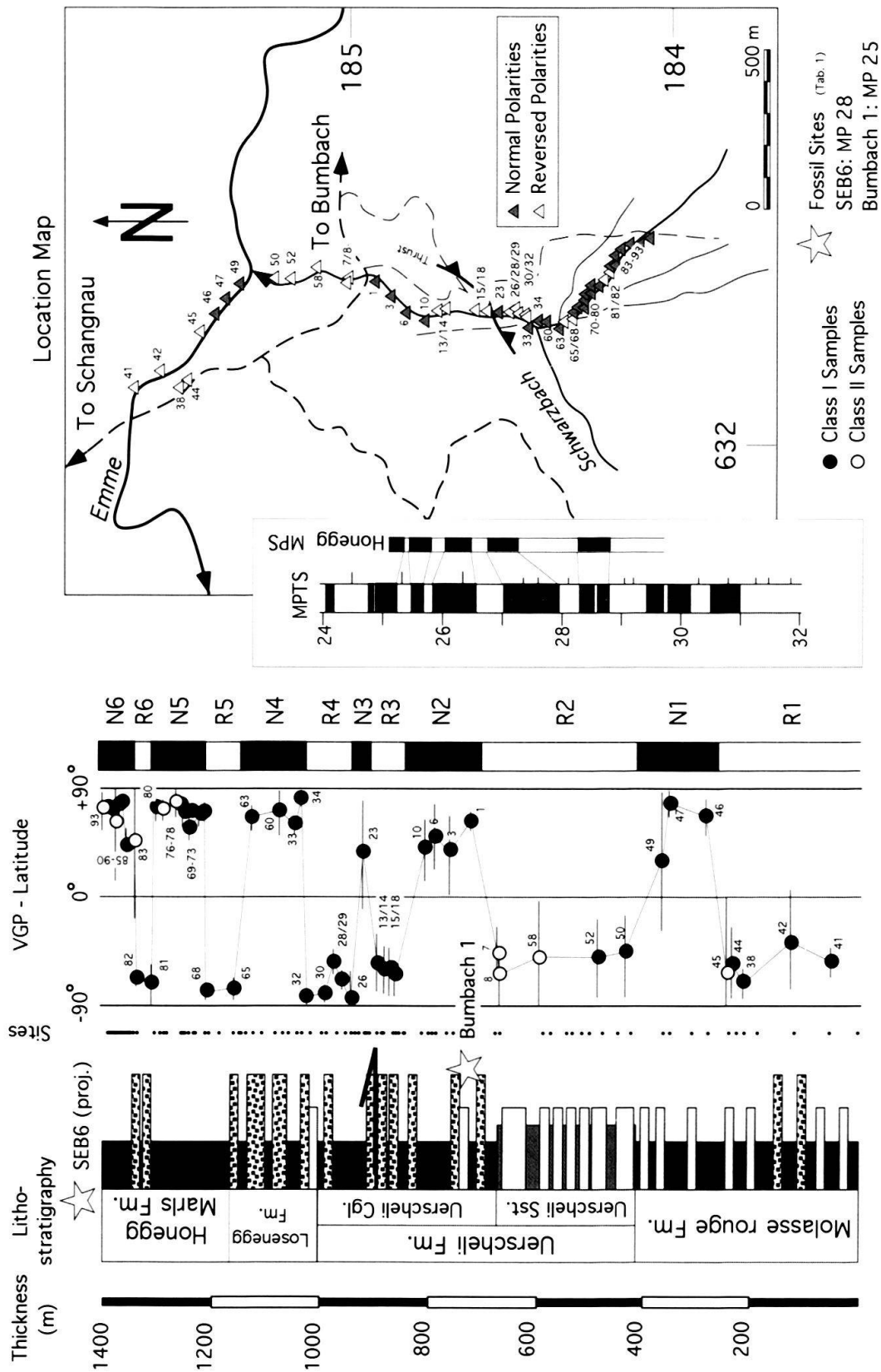


Fig. 9. Magnetostratigraphy of the Honegg section. For legend see Fig. 13.

Magnetic samples were collected from a total of 95 sites, including organic rich marls of the UMM and highly oxidized silt- and mudstones of the USM. 52% of the samples had to be discarded either because of weak and unstable magnetic signals or because of mixed polarities. Eleven magnetozones are defined, each based on two or more class I and class II sites, with the exception of N3, which is characterized by one class I site. The resultant magnetostratigraphy has a distinctive pattern characterized by a long reversed period (R3–R4) with a set of three short reversals above and below. This characteristic succession of reversals correlates well with chrons 11 and 10 of the MPTS (Fig. 11). The very short normal interval N3 is interpreted as cryptochron (Cande & Kent, 1992) or may represent a remagnetized site. This correlation implies continuous sedimentation with no erosional unconformity between UMM and USM, a conclusion which is supported by sedimentological studies (Diem, 1986).

The 1400-m-thick Honegg section (Fig. 9) is made up exclusively of USM. The lower part, consisting of the Molasse rouge Formation and Uerscheli Sandstone, correlates lithostratigraphically with the upper part of the nearby Marbach section (Fig. 3). Stratigraphically higher units include a 340-m-thick alternating series of conglomerates and mudstones, the Uerscheli Conglomerate, the dominantly conglomeratic Losenegg Formation and the Honegg Marls Formation (Fig. 9). Fossil sites in the Uerscheli Conglomerate (site Bumbach 1) and in the Honegg Marls Formation six kilometers west of the Honegg section (number 10, Fig. 3) suggest an age range from MP25 to MP28 for the studied section.

92 sites were collected in the Honegg section for magnetostratigraphy, and 53 of them define 12 magnetozones. All except one of these magnetozones (N3) are based on at least two class I sites. A fault of unknown throw that cuts the section at the base of site 23 is interpreted to repeat N2 and R3 by N3 and R4, respectively. The correlation of the Honegg MPS with the MPTS is guided by the biostratigraphic range which indicates that the section spans almost the whole Chattian, and by the predominantly reversed lower and normal upper parts of the magnetostratigraphy. This suggests a correlation with chrons 10 to 7 (Fig. 11). The very short reversals 10n.1r and 8n.1r are missing probably due to a low sample density. This correlation implies that the units at the top of the Marbach section and at the base of the Honegg section, the Molasse rouge Formation and the Uerscheli Sandstone, respectively, are isochronous. Moreover, this correlation indicates highly variable accumulation rates for the Honegg section.

The Prässerebach section is a 2800-m-thick succession of Early Chattian to earliest Aquitanian coarse grained USM with two pronounced coarsening- and thickening-upward megasequences (Fig. 10). The lower megasequence begins with the Early Chattian (MP26) Granitic Molasse Formation and ends in Late Chattian (MP28) with massive conglomerates of the Thun Formation. The upper sequence ranges from Late Chattian to earliest Aquitanian and is made up of the Honegg Marls Formation, overlain by the Gitzschöpf Conglomerate. Mapped faults at the base and at the top of the section, are interpreted to repeat almost 60 m of strata each (Fig. 3a).

A total of 150 magnetic sites were collected from the Prässerebach section at intervals between 20 to 30 m in the fine grained units and between 50 to 100 m in the conglomerates. 47% of the samples were discarded because of mixed polarities or weak intensities. All except two (R2, R7) of 17 magnetozones are defined based on at least one class I and one class II site. Because the base of N7 is cut by a thrust, N6 and R7 are repeated by N7

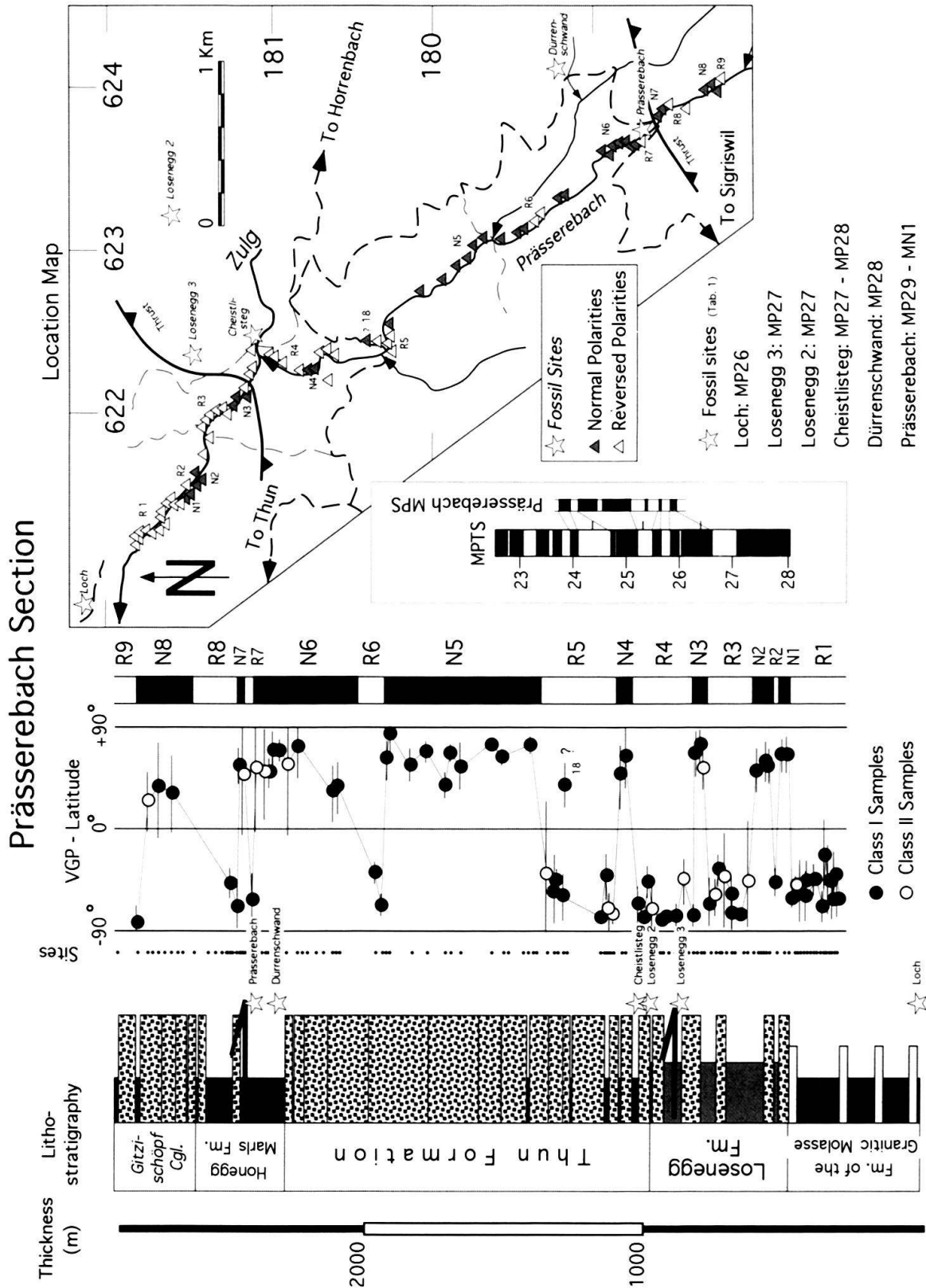


Fig. 10. Magnetostratigraphy of the Prässerebach section. For legend see Fig. 13.

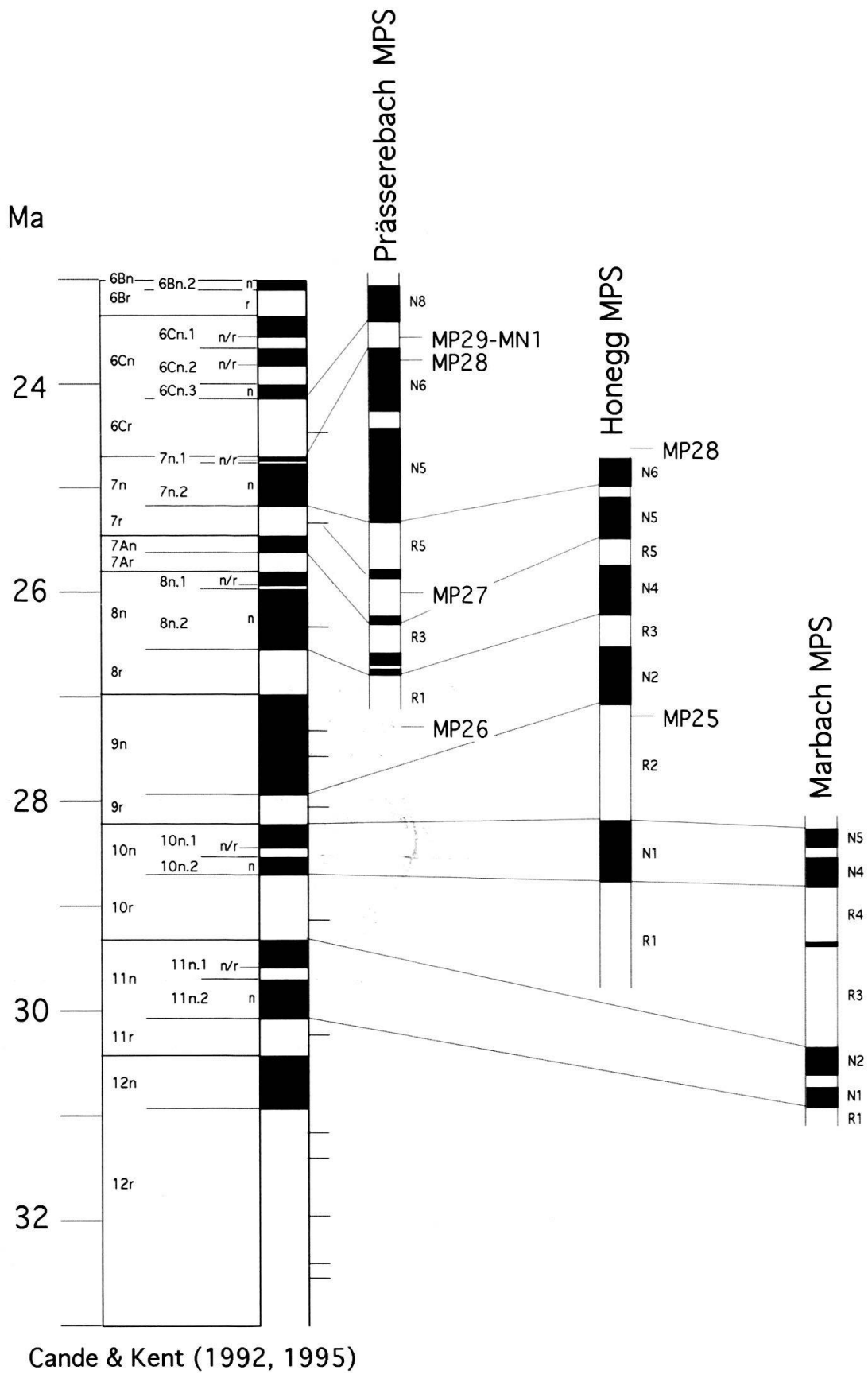


Fig. 11. Correlation of the Marbach, Honegg and Prässerebach MPS with the MPTS (left).

and R8, respectively. Furthermore, the declinations of the normal class I site 18 are strongly offset by  $90^\circ$  to the east. Resampled specimens of this site revealed mixed polarities, indicating growth of secondary magnetic minerals. Therefore, this site was not used for defining the Prässerebach reversal pattern. The mammal data indicate that the Prässerebach section spans a relatively long time period from MP26 to approximately MN1. Because of presumably varying accumulation rates as indicated by the coarsening- and thickening-upward trends, the correlation of the Prässerebach MPS with the MPTS is guided by the calibration of the faunal record in the Honegg section (Fig. 11). Consequently, the base of the Prässerebach section (R1), containing a slightly younger fauna of MP26, is correlated with the younger part of chron 8r. The Losenegg Formation and the base of the Thun Formation reveal 5 rather long reversed magnetozones, which reflect the reversal pattern between chrons 8n to 7r, implying that N4 most probably represents the wiggle of chron 7r (Fig. 11). Alternatively, R2 may represent the reversed cryptochron in chron 8n.2. In this case, N3 and N4 would correlate with chrons 8n.1 and 7An, respectively, and site 18 could represent the cryptochron in the middle of chron 7r. This correlation, however, is discarded because it implies highly varying accumulation rates for the Losenegg Formation which is in contradiction to the continuous coarsening- and thickening-upward trend (Schlunegger et al. 1993). A one-to-one correlation of the younger magnetozones (N5 to R9) with the MPTS suggests that the top of the section correlates with chron 6Cn.2r. Furthermore, MP28, represented by the fauna of Dürrenschwand (Fig. 10), correlates with chron 7n (Fig. 11), which is in good agreement with the magnetostratigraphic calibration of MP28 in the Honegg section. This calibration of the Prässerebach section supports the inference based on sedimentological data of increasing accumulation rates from the Granitic Molasse Formation to the top of the Thun Formation (first coarsening- and thickening-upward megasequence), and from the base of the Honegg Marls Formation to the top of the Gitzischöpf Conglomerate (second coarsening- and thickening-upward megasequence). Note that the brevity of the interval between magnetozones N1 to N2 suggests that the unconformity found in the Subalpine USM of the Thun area (Fig. 3b) has rather to be placed at the base than at the top of the Losenegg Formation as assumed by Schlunegger et al. (1993).

#### *Haute Savoie (Chattian-Aquitainian)*

The magnetostratigraphies established by Burbank et al. (1992) in the highly fossiliferous Chattian-Aquitainian USM in Haute Savoie (Fig. 1) were correlated with the MPTS of Berggren et al. (1985), which differs slightly from recent versions of the MPTS by Cande & Kent (1992, 1995). Differences between both polarity time scales exist for the Aquitainian chronology, so that the correlation of the Findreuse MPS as suggested by Burbank et al. (1992) needs to be reinterpreted. A succession of two normal magnetozones (N3, N4) interrupted by a very short reversal is used as fingerprint to correlate the Findreuse MPS with the MPTS of Cande & Kent (1992, 1995). On this basis, the interval from N3 to N4 is assigned to chron 6Bn (Fig. 12) instead of 6Cn.2n to 6Cn.1n as suggested by Burbank et al. (1992). The magnetostratigraphic pattern of the upper part of the Findreuse section allows a correlation which ranges from chrons 6AAr to 6An.2n of the MPTS (Fig. 12). The base of the Findreuse section (R1) may be correlated with either chron 6Cr or 6Cn.2r. The latter correlation is less likely because it would imply a high sedimentation

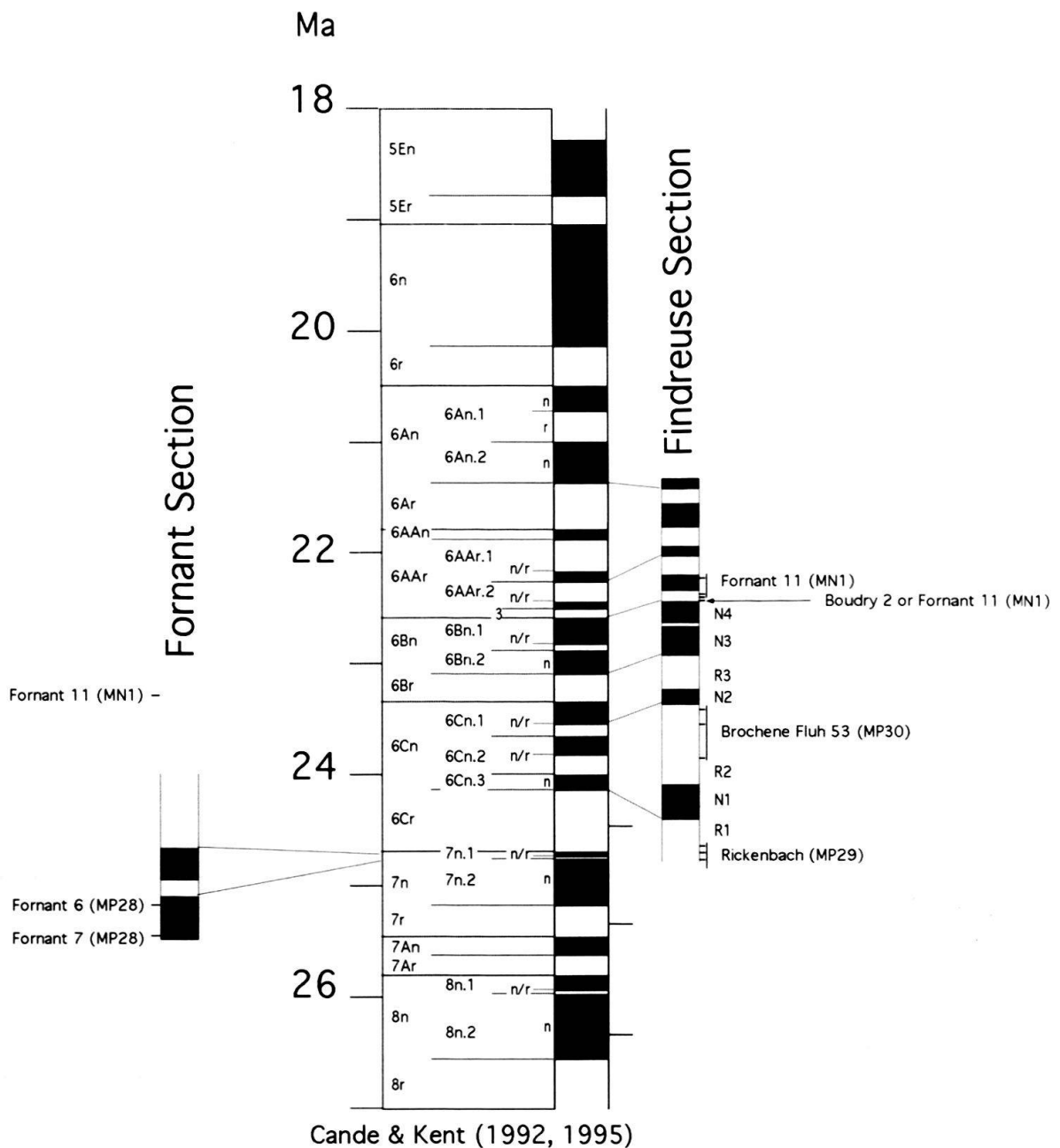


Fig. 12. Recalibration of the Fornant and Findreuse sections.

rate for both braided stream and the overlying lacustrine to palustrine limestone and marl facies. Although this correlation of the top and base of the section causes no contradictions, there remains a problem of how to correlate R2 to R3 with the MPTS. The normal polarity interval N2 can either be linked up with chron 6Cn.1n or 6Cn.2n. Both correlations imply that a normal polarity was missed due to sampling gaps in the section (see Fig. 5 in Burbank et al., 1992). The first correlation which is shown on figure 12 is preferred because it results in a smoother accumulation rate curve.

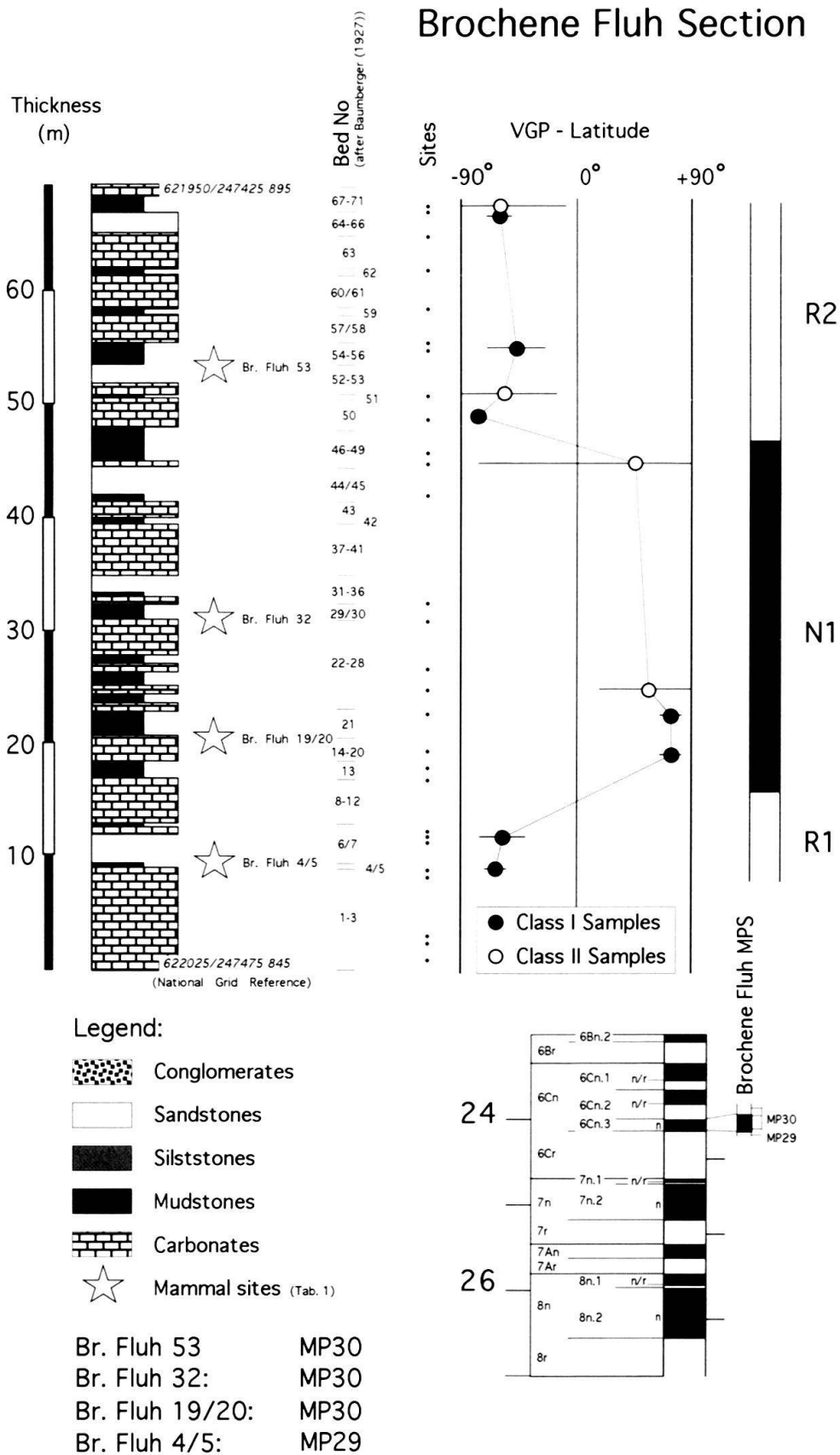


Fig. 13. Magnetostratigraphy of the Brochene Fluh section.



### *Brochene Fluh section (latest Chattian)*

The Brochene Fluh section is a 70-m-thick succession of uppermost Chattian fossiliferous lacustrine carbonates (Fig. 13). It rests unconformably on Mesozoic sediments of the Jura Mountains. A detailed lithostratigraphic description of this section was published by Baumberger (1927).

28 sites were sampled and analyzed for magnetostratigraphy, and three magnetozones are defined, each of which contains at least two class I sites. 60% of the samples had to be discarded because of weak intensities and unstable magnetic directions. Because of the thinness of the section and the presence of only 3 magnetozones, correlation is guided primarily by the faunal record and by comparison with the Findreuse magnetostratigraphy. The base of both sections is dated with MP29, which is correlated with chron 6Cr (Fig. 12, 13). The presence of four mammal levels, representing three succeeding mammal assemblage zones and recording evolutionary transitions (Engesser 1990), suggests continuous accumulation. We therefore correlate the Brochene Fluh MPS with chrons 6Cr to 6Cn.2r (Fig. 13).

### *Napf area (Aquitanian to Langhian)*

Three sections were measured and sampled for magnetostratigraphy in the Napf area (Fig. 4). The rocks are distal Aquitanian fluvial clastic strata of the USM (Fischenbach section) and Burdigalian to Langhian conglomerates of the OSM (Napf sections), which partly represent a continental equivalent of the OMM (Matter 1964; Keller 1989; Hurni 1991).

The Fischenbach section (Fig. 14) consists of a 780-m-thick succession of sandstones and siltstones (Granitic Molasse Formation). As outlined in Schlunegger (1995), sedimentation within this unit was interrupted by two major erosional events. Truncation of seismic reflectors in a seismic line 10 to 15 kilometers north of the Fischenbach section reveals that at least 100 m of USM strata were removed prior to the Burdigalian transgression. A second erosional gap with some 200 m missing occurs ~450 m below the base of the OMM.

120 sites were sampled and analyzed for magnetostratigraphy, and only 5% were discarded because of mixed polarities. The good quality of the magnetic data allowed identification of 10 magnetozones containing at least one class I and one class II site. The correlation of the Fischenbach MPS with the MPTS is constrained by a faunal datum, indicating either Fornant 11 or La Chaux, i. e. early Aquitanian, and the irregular and characteristic magnetic pattern of the lower part of the section (Fig. 14). The magnetic pattern indicates an age range from chron 6Cn.1r to 6AAr.2r. The magnetostratigraphy of the upper part of the section comprises four magnetozones (Fig. 14). The rather non-distinctive magnetic pattern allows three different possibilities for correlating the Fischenbach MPS with the MPTS, resulting in time gaps of different lengths: (i) 300 kyr if N4 to N5 is correlated with 6AAr to 6An.2n, (ii) 900 kyr if correlated with 6An.2n to 6An.1n, and (iii) 1600 kyr if calibrated with 6An.1n to 6n. In the context of the average accumulation rate of 300 m/Ma determined from the lower part of the section interpretations (i) and (iii) are discarded because they imply unreasonably high and low accumulation rates of at least 670 m/Ma and 125 m/Ma for the eroded 200 m of strata, respectively.

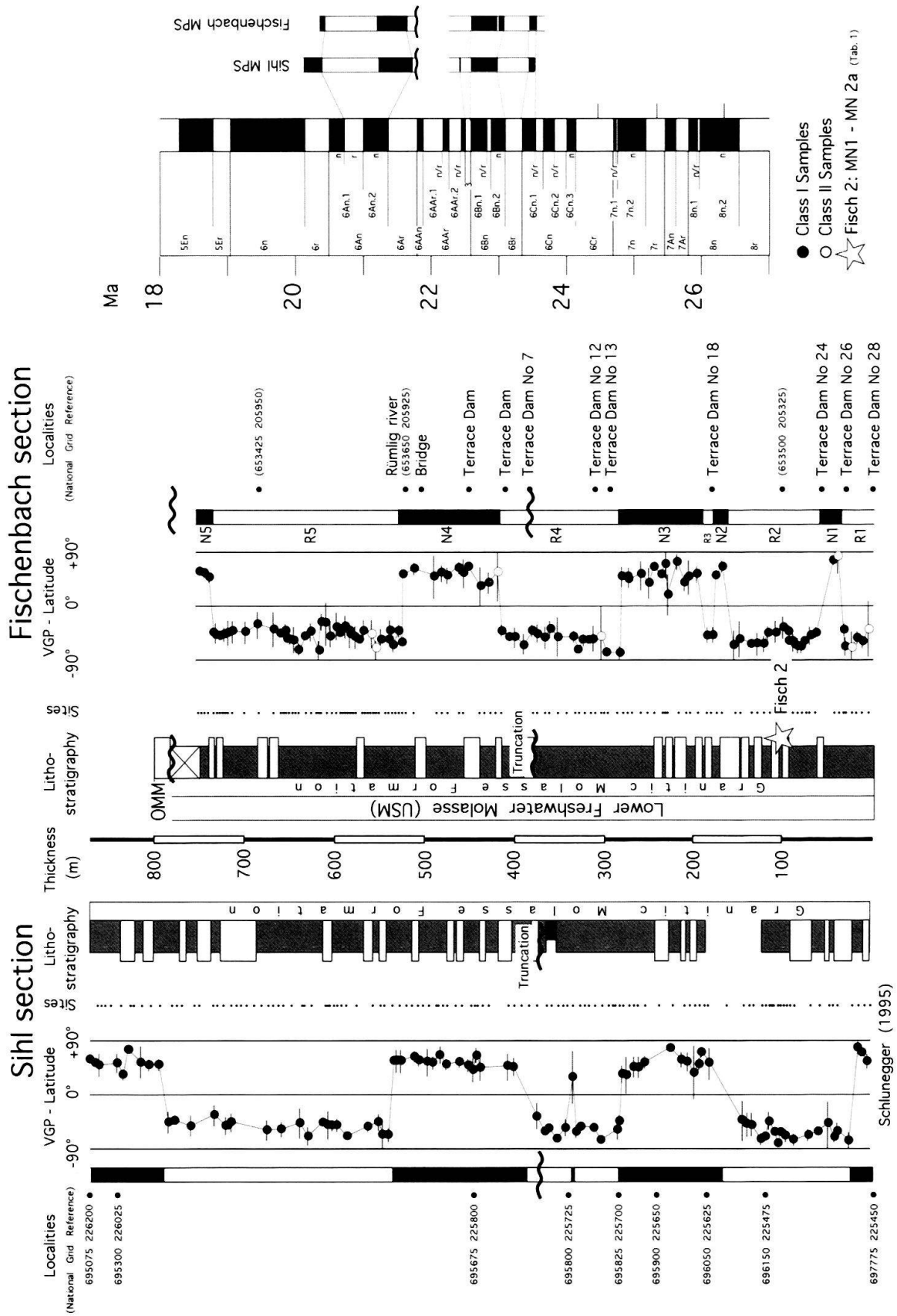


Fig 14. Magnetostratigraphy of the Fischenbach and Sihl sections. For legend see Fig. 13.

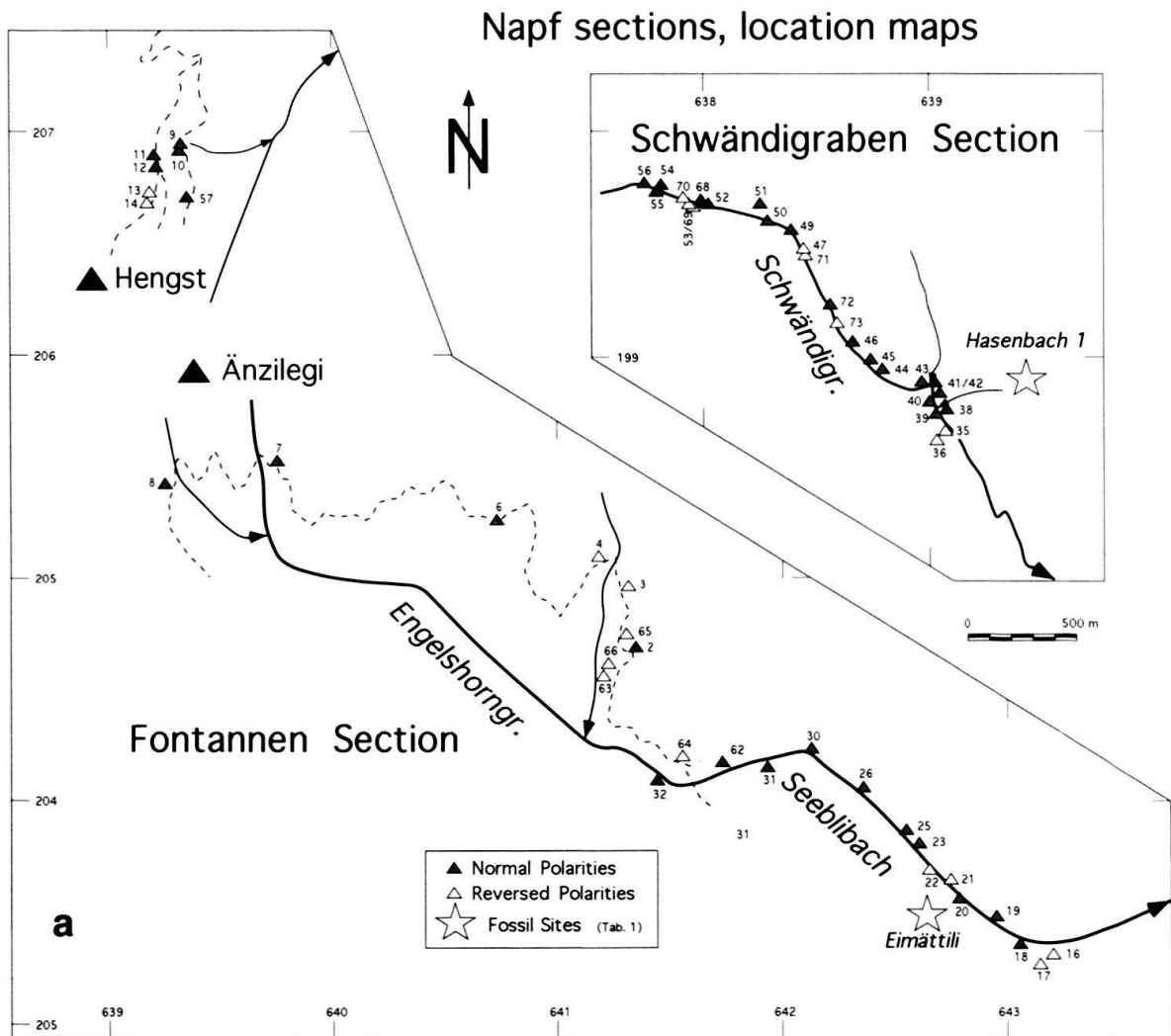
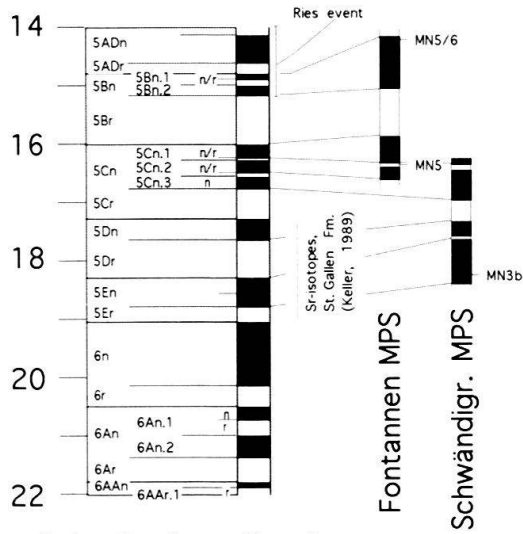


Fig. 15. Magnetostratigraphy of the Napf sections with a) location map and b) reconstruction of the Napf MPS and correlation with the MPTS (see next page).

The second sampled section in the Granitic Molasse Formation along the Sihl river 50 kilometers to the east of Fischenbach (Fig. 1) has a magnetostratigraphic pattern which is identical to the Fischenbach MPS (Fig. 14). Note that in the Sihl section the short normal magnetozone 6AAr.2n which is missing in the Fischenbach, is present.

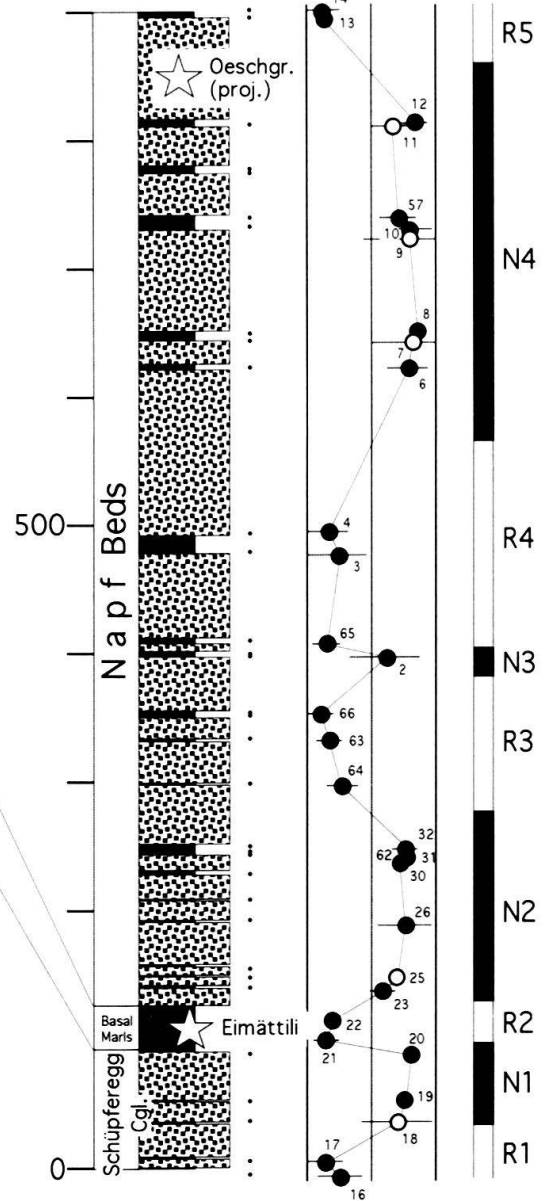
In the Napf area, the Schwändigraben and Fontannen sections, with an overlap of 150 m, form a composite succession ranging from Burdigalian to Langhian (Fig. 15). They consist of 116 m of alternating conglomerates, sandstones and marls (Luzern Formation, OMM), overlain by a roughly 1400 m thick succession of mainly massive conglomerates (Schüpferegg Cgl., Napf Beds), which are interbedded with green lacustrine marls and siltstones (Basal Marls).

### Napf Sections



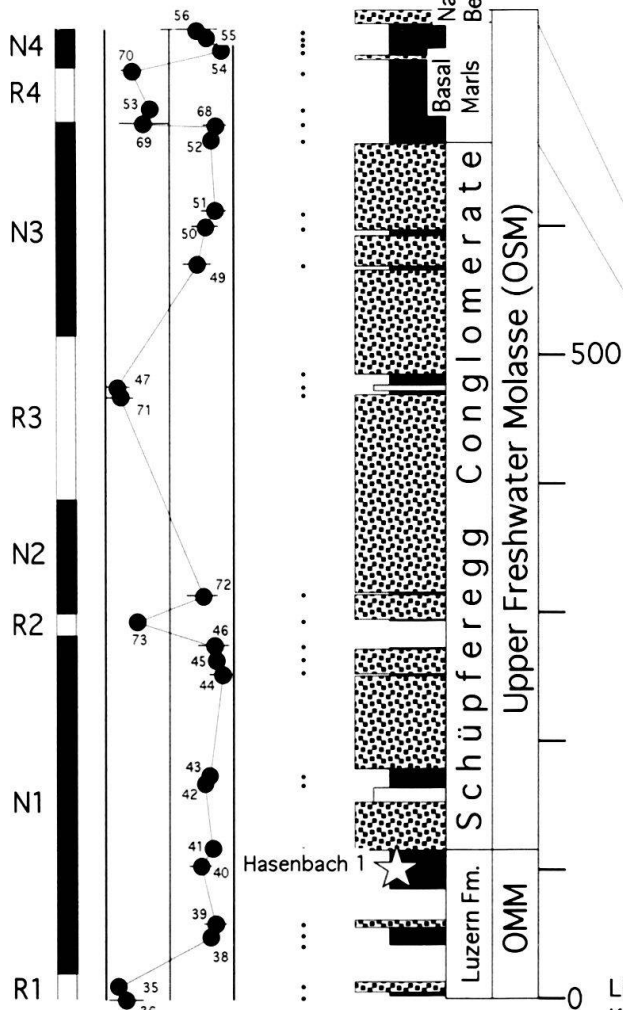
### Fontannen Section

Thickness (m) Strat. Sites VGP-Latitude (-90° 0° +90°)



### Schwändigr. Section

VGP-Latitude (-90° 0° +90°) Sites Strat.



- Class I Samples
- Class II Samples
- ☆ Mammal Sites (Tab. 1)
- Hasenbach 1: MN3b
- Eimättli: MN5
- Oeschgraben: MN5/6

Lithostratigraphy modified after Matter (1964) & Keller (1989)

**b**

A total of 73 magnetic sites were sampled, and 75% of the samples allowed identification of 17 magnetozones. Each zone is defined by at least two class I sites with the exceptions of R2 and N2 of the Schwändigraben section and N3 of the Fontannen section. Site 2, which defines N3 in the Fontannen section, shows strongly rotated declinations, leading to a shallow VGP-latitude. In addition, the magnetic directions of the six samples are highly variable, resulting in a large polar error and uncertain polarity. Therefore, this site is ignored in our correlation.

The correlation of the composite Napf section is constrained by the Ries meteorite impact, dated radiometrically ( $14.6 \pm 0.6$  Ma), and by a mammal site (MN6) in the oldest lacustrine sediments of the crater (Gall 1980; Stöfler 1977; Heizmann & Fahlbusch 1983; Engelhardt & Graup 1984; Lemcke 1988). Because the uppermost Napf Beds also contain a mammal fauna of MN5/6, the Ries event represents an upper absolute age limit. The lower part of the section is dated with MN3b, and, therefore, the Schüpferegg Conglomerate is contemporaneous with the marine St. Gallen Formation (Fig. 4). Using strontium isotope chemostratigraphy, Keller (1989) dated this unit with the range from NN3 to lower NN4, which corresponds to chrons 5E to 5D (Berggren et al., in press.). As a result, the Napf magnetostratigraphies must correlate with the portion of the MPTS from approximately 19 to 15 Ma. Because of the uncertainty in the radiometric date (600 kyr), it seems that the top of N4 in the Fontannen section could correlate with both the top of 5Bn.1 and 5Bn.2 (Fig. 15). Given this range and the presently defined ages of the MPTS magnetozones (Cande & Kent 1992, 1995), the distinctive pattern of reversals of the Napf section correlates well with the MPTS (Fig. 15). Note that chron 5Dr, encompassing approximately 650 kyr, is represented in the Schwändigraben section by a very short reversed magnetozone (R2), because of erosion related to lowering of base-level during regression, as identified by Keller (1989) farther to the east in the middle of the St. Gallen Formation.

## Discussion

### *Magnetic samples processing*

The success of demagnetization in removing secondary magnetization determines the quality of the resulting magnetostratigraphies. Detailed demagnetization pilot studies carried out on marls, mudstones and siltstones from the different depositional environments revealed three magnetic components: (i) a low temperature magnetic signal, removed at 250°C, which is probably carried by titanomagnetite, (ii) a magnetic signal in the 250–550°C temperature window related to magnetite group minerals and (iii) a magnetization remaining at high temperatures, which is most probably carried by hematite. Stepwise thermal demagnetization within the 250–550°C temperature window shows a steady decrease in intensity and stable inclination and declination vectors which indicate that reliable characteristic remanences have been found. Magnetic directions in the lower and upper temperature windows are unstable and often show opposite and mixed polarities. Organic-rich lithologies such as marine marls and lacustrine carbonates revealed increased susceptibilities at 400°C probably due to oxidation of sulfide minerals. Such samples displayed more stable demagnetization vectors when processed within a 250–350°C temperature window. Excellent magnetic results were obtained in the Aquita-

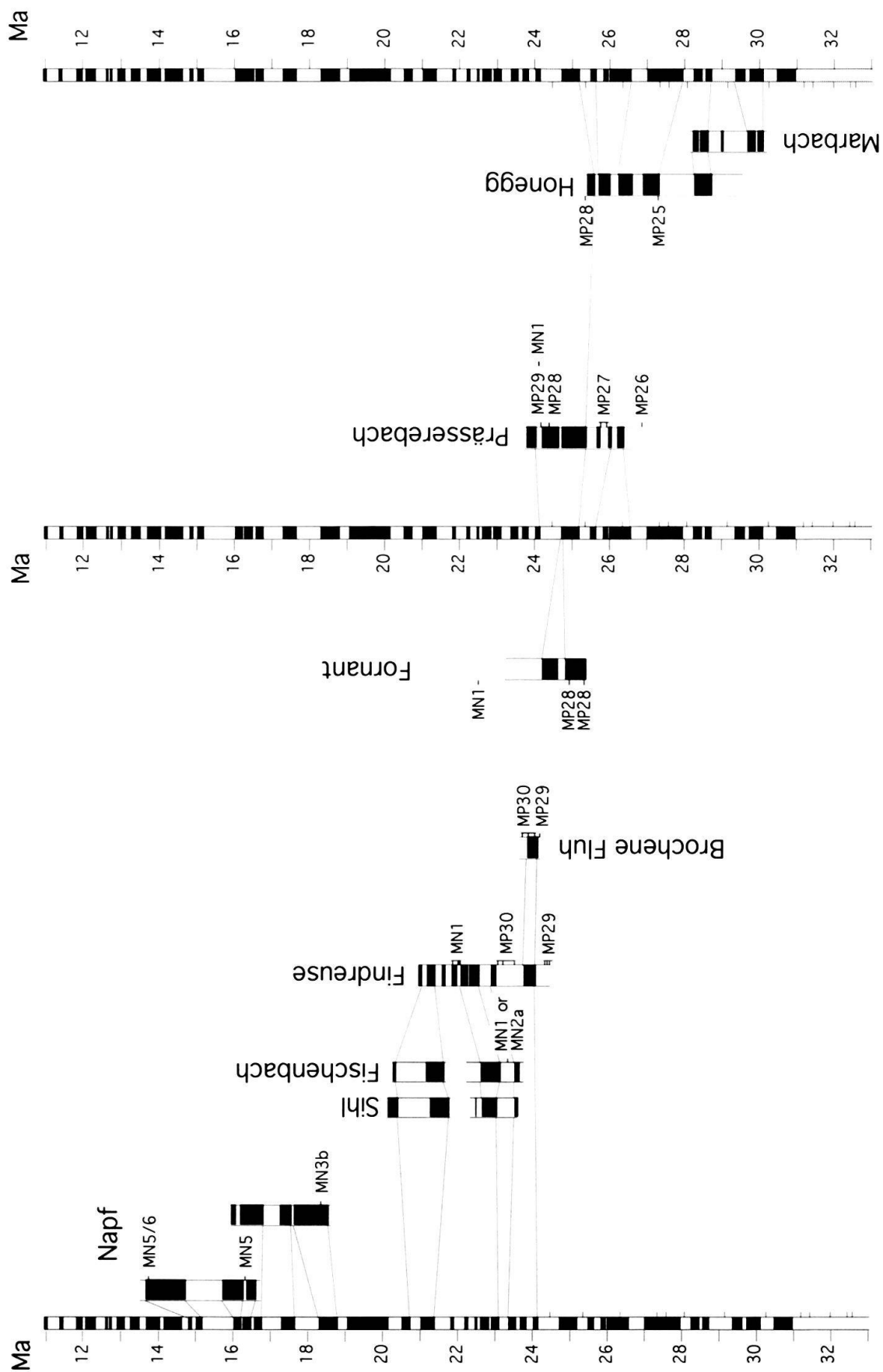


Fig. 16. Best fit correlation of the analyzed sections with the MP/MS of Cande & Kent (1992, 1995).

nian to Langhian deposits of the Plateau Molasse, where only 5 to 25% of the samples had to be discarded because of mixed polarities. In the Chattian Subalpine Molasse, however, the magnetic signal was often less clear, and ca. 50% of the samples were rejected because of mixed polarities or weak magnetic intensities. Lacustrine specimens collected at the feather edge of the basin revealed very weak intensities, so that 60% of the samples could not be used for defining the reversal pattern.

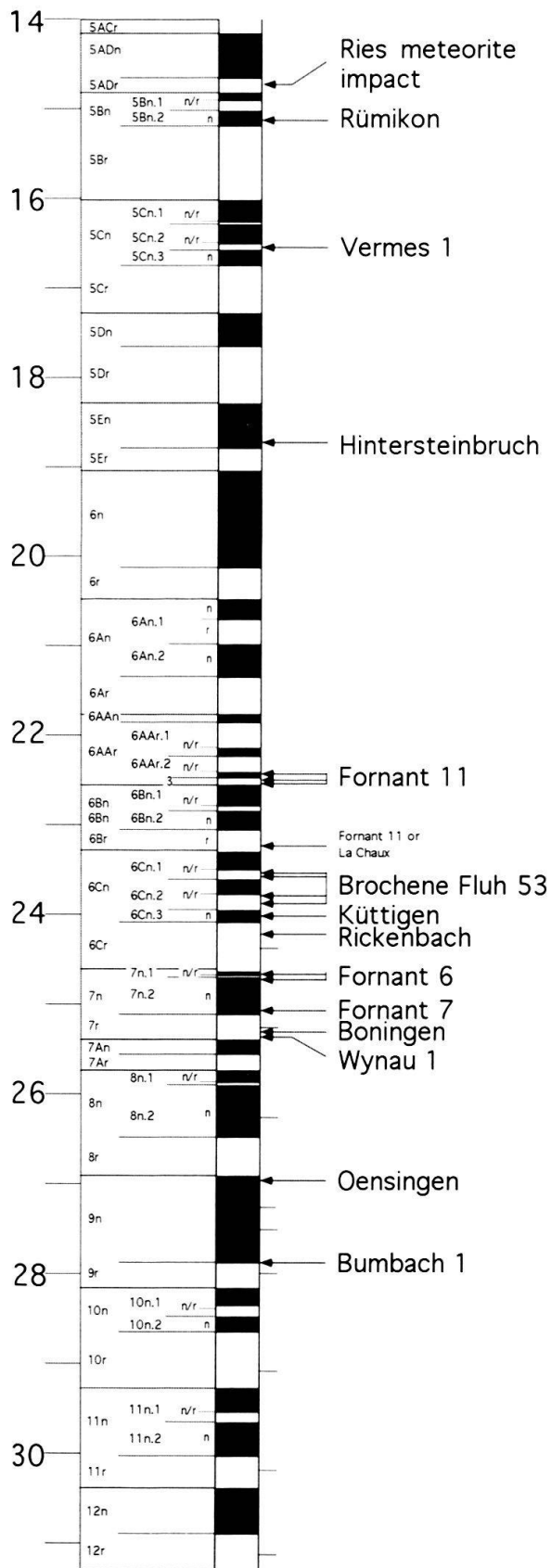
#### *Correlation of magnetic sections*

In many studies magnetic sections are correlated assuming progressive and regular subsidence (for details see Talling & Burbank 1993). The results of this study, however, indicate that in both proximal and distal portions of the Molasse Basin unconformities spanning time intervals of at least 500 kyr may occur. Furthermore, accumulation rates change significantly within a very short time period, resulting in a strong distortion of the reversal pattern. In this paper we are using a combination of sedimentological, seismic, biostratigraphic, radiometric and geochemical data to correlate the magnetostratigraphies. In order to avoid circular reasoning, we use the faunal record strictly to establish the biostratigraphic and gross temporal framework. Characteristic successions of magnetic polarities were then used as fingerprints for the final correlation of MPS with the MPTS, provided that mammal and sedimentological data suggest continuous sedimentation. Nevertheless, an unconformity is present in the USM and another one exists at the base of the OMM, both of which can be seen only on seismic lines across the Plateau Molasse. The integrated approach used here improves the correlation quality of the analyzed sections significantly, and correlations other than those shown on figure 16 seem to cause major contradictions among the sections.

#### *Calibration of mammalian assemblage zones and Molasse groups*

The new correlation of the local MPS with the MPTS given here calibrates for the first time the mammalian stages from Early Chattian to the Langhian in the Molasse Basin. Based on the correlation presented in figure 16, one can place the mammal assemblage zones into the chronological framework of the MPTS (Fig. 17). Despite the precise chronology given by the magnetostratigraphies of eight sections, the application of the correlation chart (Fig. 17) has four limitations: (i) whereas in the Chattian to early Aquitanian almost all assemblage zones were found in the studied sections, only few were directly calibrated in the upper Aquitanian to Langhian, (ii) assemblage zone boundaries cannot be calibrated precisely due to absence of appropriately spaced mammal sites, (iii) occasionally part of the magnetic pattern may be correlated in more than one way with the MPTS, and (iv) the presence of long magnetozones in the MPTS may prevent accurate location of assemblage zone boundaries. Nonetheless, figure 17 shows that the average duration of the assemblage zones varies from approximately 300 kyr in the Late Chattian to roughly 800 kyr in the Aquitanian to Langhian and Early Chattian.

Our calibration of the mammal assemblage zones of the Late Chattian to early Aquitanian differs slightly from that given by Burbank et al. (1992) as a result of the introduction of new magnetozones in the recalibrated MPTS of Cande & Kent (1992, 1995). The most significant changes include the position of the boundary between the assemblage



Cande & Kent (1992, 1995)

Rümikon	MN 5/6	Langhian	M i o c e n e
Vermes 1	MN 5		
Hirschthal	b	Burdigalian	
Wattwil	a		
Hintersteinbr.	b		
Bierkeller	a		
Brüttelen 2	MN 3	Aquitanian	
Vully 1	b		
La Chaux	a		
Fornant 11	MN 1	Late Ch.	
Boudry 2	MP 30/		
Br. Fluh 53	MN 0	Early Chattian	
Küttigen	MP 29		
Rickenbach	MP 28		
Fornant 6	MP 27		
Fornant 7	MP 27	O l i g o c e n e	
Boningen	MP 27		
Wynau 1	MP 26		
Mümliswil-H.	MP 26		
Oensingen	MP 26	Early Chattian	
Bumbach 1	MP 25		
Grenchen 1	MP 24		

Fig. 17. Calibration chart of the mammal assemblage zones.



zones Brochene Fluh 53 and Boudry 2, now located at the base of chron 6Cn.1n at ca. 23.5 Ma and the longer duration of the assemblage zones Fornant 6 (MP28) and Rickenbach (MP29). These zones now last on average 330 kyr as opposed to 200 kyr in Burbank et al. (1992). These authors postulated large variations in the duration of the Late Chattian mammal assemblage zones whereas we conclude that they represent roughly equal time intervals. Furthermore, this study reveals that the Palaeogene/Neogene boundary should be placed within the assemblage zone of Brochene Fluh 53 (Fig. 17) rather than at its top as suggested by Engesser (1990) in order to agree with the chronology of the type section of the Palaeogene/Neogene boundary (Lemme section, NW-Italy). For this section Steininger (1994) recommended placing the Palaeogene/Neogene boundary at the base of chron 6Cn.2n at 23.8 Ma.

Major differences also exist between the results of this study and the chronologic data from the Calatayud-Teruel basin (Central Spain). The magnetostratigraphies established in the Spanish basin by Krijgsman et al. (1994) suggest that the MN4/MN5 boundary coincides with chrons 5ACr or 5ADn of Cande & Kent (1992, 1995), which is approximately 2 Ma years younger compared to our results. The reason for these discrepancies probably lies in the different correlations of the Swiss and Spanish mammal zonations with the MP/MN scheme. Furthermore, magnetostratigraphic chronologies established in the Ebro basin (Torrente de Cinca section) resulted in a slightly different calibration of the Early Chattian MP/MN zonation than presented in this paper (Augusti et al. 1994; Barberà et al. 1994). However, as pointed out by these authors, the correlation of the Torrente de Cinca MPS to the MPTS is ambiguous.

The new magnetic stratigraphic calibrations presented here also greatly improve the temporal control of the depositional record in the North Alpine foreland during the period from 30 to 15 Ma. The new chronology suggests that the UMM regression occurred in central Switzerland at 30 Ma, coinciding with an eustatic sea level fall in the curve of Haq et al. (1987). However, there is clear stratigraphic evidence that in areas where fan deltas prograded into the UMM sea, the UMM/USM boundary is much older and the contact is therefore strongly time transgressive (Schlunegger 1995; Kempf, pers. comm. 1995).

The transgression of the OMM sea was also heterochronous, as indicated by both biostratigraphic data (Keller 1989; Berger 1992) and the magnetostratigraphic calibration of the top of the USM. In Haute Savoie the transgression occurred at ca. 21 Ma and in the Napf area at 20 Ma, confirming the findings of Keller (1989) and Berger (1992) that the narrow, perialpine seaway expanded from west to east, finally linking the Tethys and Paratethys.

As in the UMM, the transition from marine OMM to continental OSM is earlier in areas of fan deltas than outside these areas. For example, in the center of the Napf fan, OSM conglomerates rest directly on USM with no marine OMM in between (Haldermann et al. 1980; Schlunegger et al. 1993). Some 10 kilometers farther to the east, however, in the Schwändigraben section (Fig. 15), the OMM regression occurred at ca. 18.7 Ma as compared to ca. 17 Ma in eastern Switzerland (MN4/5, Keller 1989).

## Conclusions

The new magnetostratigraphic chronologies presented here for eight stratigraphic sections in the North Alpine foreland basin provide the most detailed and precise temporal calibration that is presently available of the faunal and depositional record for the area. The magnetic chronologies establish time limits for the detailed mammal biozonation previously defined in the Molasse Basin and allow correlation with both the mammalian record of other continental basins and with the established marine biozonations. The duration of the assemblage zones varies from approximately 300 kyr in the Late Chattian to ca. 800 kyr in the Aquitanian to Langhian and Early Chattian.

The boundaries between the four major lithostratigraphic groups traditionally recognized in the Molasse Basin can be generally placed at: 30 Ma for the UMM/USM, 20 Ma for the USM/OMM and 17 Ma for the OMM/OSM. These limits are strongly time-transgressive, however, and may vary by at least 3 Ma.

The chronologic calibration of mammal assemblage zones and of the architectural pattern of the Molasse will greatly improve the reconstruction of the causal relationships between tectonic events in the Alpine orogen and the response in the foreland basin. Furthermore, chronologic constraints will permit the calculation of the sediment flux into the foreland and thus the reconstruction of the denudation history of the Alpine hinterland. As pointed out by Beaumont (1981), Jordan (1981), Flemings & Jordan (1989, 1990) and Sinclair et al. (1991) foreland-basin chronologies, sediment flux and subsidence rates are crucial temporal parameters for understanding the interaction of Alpine orogeny and foreland basin evolution.

## Acknowledgements

We would like to thank F. Wiedenmayer who helped with obtaining the large amounts of material required for micromammal studies. The help of S. Lund for advising us in interpreting the demagnetization data is greatly acknowledged. Thanks go to H. Bärtschi for technical instructions and to S. Henyey for processing numerous Napf samples. The help of S. Burns with the English is kindly acknowledged. Special thanks go to O. Kempf for fruitful discussions. Finally, F. Schlunegger thanks his colleagues who acted as assistants and climbing instructors. Partial support for this research was provided by the Swiss National Science Foundation (grant no. 21-36219.91).

## REFERENCES

- AGUSTI, J., BARBERO, X., CABRERA, L., PARES, J.M. & LLENAS, M. 1994: Magnetobiostratigraphy of the Oligocene-Miocene transition in the Ebro Basin (eastern Spain): state of the art. *Münchner Geowiss. Abh. (A)* 26, 161–172.
- BARBERA, X., PARES, J.M., CABRERA, L. & ANADUN, P. 1994: High-resolution magnetic stratigraphy across the Oligocene-Miocene boundary in an alluvial-lacustrine succession (Ebro Basin, northeast Spain). *Phys. Earth Planet. Inter.* 85, 181–193.
- BAUMBERGER, E. 1927: Die stampischen Bildungen der Nordwestschweiz und ihrer Nachbargebiete mit besonderer Berücksichtigung der Molluskenfaunen. *Eclogae geol. Helv.* 20, 533–578.
- BEAUMONT, C. 1981: The evolution of sedimentary basins on a visco-elastic lithosphere. Theory and examples. *Geophys. J. r. astron. Soc.* 55, 471–497.
- BECK, P. & RUTSCH, R.F. 1949: Geologischer Atlas der Schweiz 1:25'000, Bl. Münsingen-Konolfingen-Gerzensee-Heimberg (Nr. 21). Schweiz. geol. Komm.
- BENTHAM, P. A. 1992: The tectonostratigraphic development of the western oblique ramp of the south-central Pyrenean thrust system, northern Spain. Ph.D. thesis, University of Southern California, Los Angeles.
- BERGGREN, W.A., KENT, D.V., FLYNN, J.J. & VAN COUVERING, J.A. 1985: Cenozoic geochronology. *Bull. geol. Soc. Amer.* 96, 1407–1418.
- BERGGREN, W.A., KENT, D.V., SWISHER, C.C. & AUBRY, M.-P. 1995: A revised Cenozoic geochronology and chronostratigraphy. In: *Geochronology, Time Scales and Global Stratigraphic Correlations*. (Ed. by BERGGREN, W. A., KENT, D.V., AUBRY, M.-P. & HARDENBOL, J.). *Spec. Publ. Soc. econ. Paleont. Mineral.* 54, 17–28.
- BERGER, J.P. 1990: Tableau comparatif des corrélations de l'Oligo-Miocène et position stratigraphique de la Molasse suisse. *Abstr. Réunion Soc. géol. Suisse, Genève*.
- 1992: Correlative chart of the European Oligocene and Miocene: Applications to the Swiss Molasse Basin. *Eclogae geol. Helv.* 85, 573–609.
- BERLI, S. 1985: Die Geologie des Sommersberges (Kantone St. Gallen und Appenzell). *Ber. St. gall. natf. Ges.* 82, 112–145.
- BOLLIGER, T. 1992: Kleinsäugerstratigraphie in der lithologischen Abfolge der miozänen Hörnlischüttung (Ostschweiz) von MN3 bis MN7. *Eclogae geol. Helv.* 85, 961–1000.
- BRENNAN, W.J. 1993: Origin and modification of magnetic fabric in fine-grained sediment by depositional and post depositional processes. In: *Applications of paleomagnetism to sedimentary geology*. (Ed. by AISSAOUI, D.M. McNEILL, D.F. & HURLEY, N.F.). *Spec. Publ. Soc. econ. Paleont. Mineral.* 49, 17–28.
- BURBANK, D.W., ENGESSER, B., MATTER, A. & WEIDMANN, M. 1992: Magnetostratigraphic chronology, mammalian faunas, and stratigraphic evolution of the Lower Freshwater Molasse, Haute-Savoie, France. *Eclogae geol. Helv.* 85, 399–431.
- BURKHARD, M. 1990: Aspects of the large-scale Miocene deformation in the most external part of the Swiss Alps (Subalpine Molasse to Jura fold belt). *Eclogae geol. Helv.* 83, 559–583.
- BUTLER, R.F. 1992: *Paleomagnetism*. Blackwell Sci. Publ., Boston.
- CANDE, S.C. & KENT, D.V. 1992: A new geomagnetic polarity timescale for the late Cretaceous and Cenozoic. *J. geophys. Res.* 97, 13917–13951.
- 1995: Revised calibration of the geomagnetic polarity timescale for the Late Cretaceous and Cenozoic. *J. geophys. Res.* 100, 6093–6095.
- DIEM, B. 1986: die Untere Meeresmolasse zwischen der Saane (Westschweiz) und der Ammer (Oberbayern). *Eclogae geol. Helv.* 79, 493–559.
- ENGELHARDT, W.V. & GRAUP, G. 1984: Suevite of the Ries crater, Germany: Source rocks and implications for cratering mechanics. *Geol. Rdsch.* 73, 447–481.
- ENGESSER, B. 1990: Die Eomyidae (Rodentia, Mammalia) der Molasse der Schweiz und Savoyens. *Systematik und Biostratigraphie. Schweiz. paläont. Abh.* 112.
- ENGESSER, B. & MAYO, N. A. 1987: A biozonation of the Lower Freshwater Molasse (Oligocene and Agenian) of Switzerland and Savoy on the basis of fossil mammals. *Münchner Geowiss. Abh. (A)* 10, 67–84.
- FAHLBUSCH, V. 1991: The meaning of MN-Zonation: consideration for a subdivision of the European continental Tertiary using mammals. *Newsl. Stratigr.* 24, 159–173.
- FISHER, R.A. 1953: Dispersion on a sphere. *Proc. r. Soc. London A217*, 295–305.
- FLEMINGS, P.B. & JORDAN, T.E. 1989: A synthetic stratigraphic model of foreland basin development. *J. geophys. Res.* 94, 3851–3866.

- 1990: Stratigraphic modelling of foreland basins: interpreting thrust deformation and lithospheric rheology. *Geology* 18, 430–434.
- GALL, H. 1980: Das Nördlinger Ries, ein Meteoritenkrater. Hrsg. Freunde Bayer. Staatsslg. Paläont. u. hist. Geol., e.V., 4. Aufl.
- GASSER, U. 1966: Sedimentologische Untersuchungen in der äusseren Zone der subalpinen Molasse des Entlebuch (Kt. Luzern): *Eclogae geol. Helv.* 59, 723–772.
- 1968: Die innere Zone der subalpinen Molasse des Entlebuch (Kt. Luzern), *Geologie und Sedimentologie. Eclogae geol. Helv.* 61, 229–313.
- HALDEMANN, E.G., HAUS, H.A., HOLLIGER, A., LIECHTI, W., RUTSCH, R.F. & DELLA VALLE, G. 1980: Geologischer Atlas der Schweiz 1:25'000, Blatt 1188 Eggwil (Nr. 75). Schweiz. geol. Komm.
- HAO, B.U., HARDENBOL, J. & VAIL, P.R. 1987: Chronology of fluctuating sea levels since the Triassic. *Science* 235, 1156–1167.
- HAUS, H. 1937: Geologie der Gegend von Schangnau im oberen Emmental (Kt. Bern). Ein Beitrag zur Stratigraphie und Tektonik der subalpinen Molasse und des Alpenrandes. *Beitr. geol. Karte Schweiz [NF] 75*. Schweiz. geol. Komm.
- HAWTHORNE, T.B. & MCKENZIE, J.D. 1993: Biogenic magnetite: Authigenesis and diagenesis with changing redox conditions. In: *Applications of paleomagnetism to sedimentary geology*. (Ed. by AISSAOUI, D.M., MCNEILL, D.F. & HURLEY, N.F.). *Spec. Publ. Soc. econ. Paleont. Mineral.* 49, 3–16.
- HEIZMANN, E.P.J. & FAHLBUSCH, V. 1983: Die mittelmiozäne Wirbeltierfauna vom Steinberg (Nördlinger Ries). *Mitt. Bayer. Staatsslg. Paläont. hist. Geol.* 23, 83–93.
- HOMEWOOD, P., ALLEN, P.A. & WILLIAMS, G.D. 1986: Dynamics of the Molasse Basin of western Switzerland. In: *Foreland Basins*. (Ed. by ALLEN, P.A. & HOMEWOOD P.). *Spec. Publ. int. Assoc. Sedimentol.* 8, 199–217.
- HURNI, A. 1991: Geologie und Hydrogeologie des Truebtales. Unpubl. Diploma thesis Univ. Bern.
- JORDAN, T.E. 1981: Thrust loads and foreland basin evolution, Cretaceous, western United States. *Bull. amer. Assoc. Petroleum Geol.* 65, 2506–2520.
- KARLIN, R. 1990: Magnetite diagenesis in marine sediments from the Oregon continental margin. *J. geophys. Res.* 95, 4405–4419.
- KARLIN, R. & LEVI, S. 1983: Diagenesis of magnetic minerals in recent hemipelagic sediments. *Nature* 303, 327–330.
- KELLER, B. 1989: Fazies und Stratigraphie der Oberen Meeresmolasse (Unteres Miozän) zwischen Napf und Bodensee. Unpubl. Ph.D. thesis Univ. Bern.
- KELLER, B., BLÄSI, H.-R., PLATT, N.H., MOZLEY, P.S. & MATTER, A. 1990: Sedimentäre Architektur der distalen Unteren Süsswassermolasse und ihre Beziehung zur Diagenese und den petrophysikalischen Eigenschaften am Beispiel der Bohrungen Langenthal. *Geologische Berichte No. 13*, Landeshydrologie und -geologie.
- KRIJGSMAN, W., LANGEREIS, C.G., DAAMS, R. & VAN DER MEULEN, A.J. 1994: Magnetostratigraphic dating of the middle Miocene climate change in the continental deposits of the Aragonian type area in the Calatayud-Teruel basin (Central Spain). *Earth Planet. Sci. Lett.* 128, 513–526.
- LEMCKE, K. 1988: Geologie von Bayern. – I. Teil: Das bayerische Alpenvorland vor der Eiszeit. Schweizerbart, Stuttgart.
- MATTER, A. 1964: Sedimentologische Untersuchungen im östlichen Napfgebiet (Entlebuch – Tal der Grossen Fontanne, Kt. Luzern). *Eclogae geol. Helv.* 57, 315–429.
- MATTER, A., HOMEWOOD, P., CARON, C., RIGASSI, D., VAN STUIJVENBERG, J., WEIDMANN, M. & WINKLER, W. 1980: Flysch and Molasse of western and central Switzerland, a guide book, part II. (Ed. by TRÜMPY, R.). *Schweiz. geol. Komm.*, 261–293.
- MCELHINNY, M.W. 1964: Statistical significance of the fold test in paleomagnetism. *Geophys. J. r. astron. Soc.* 8, 338–340.
- 1973: *Paleomagnetism and Plate Tectonics*. Cambridge University Press, Cambridge, 358.
- MEIN, P. 1975: Résultats du groupe des vertébrés: Biozonation du Néogène méditerranéen à partir des Mammifères. In: *Report on Activity of the RCMNS Working groups (1971–1975)*. (Ed. by SENES, J.). Bratislava, 78–81.
- 1989: Updating of MN zones. In: *European Neogene mammal chronology*. (Ed. by LINDSAY, E., FAHLBUSCH, V. & MEIN, P.). Plenum Press, New York, 73–90.
- MÖDDEN, C. 1993: Revision der Archenomyimi Schlosser (Rodentia, Mammalia) des europäischen Oberoligozän. *Schweiz. Pälont. Abb.* 115.

- MÖDDEN, C. & GAD, J. 1992: Archaeomys-Arten (Theridomorpha, Rodentia) des oberoligozänen stratigraphischen Referenz-Niveaus Boningen (Schweiz). *Eclogae geol. Helv.* 86, 947–960.
- PAVONI, N. & SCHINDLER, K. 1981: Bentonitvorkommen in der Oberen Süswassermolasse und damit zusammenhängende Probleme. *Eclogae geol. Helv.* 74, 53–64.
- PEIFFNER, O.A. 1986: Evolution of the north Alpine foreland basin in the Central Alps. In: *Foreland Basins*. (Ed. by ALLEN, P.A. & HOMEWOOD, P.). *Spec. Publ. int. Ass. Sediment* 8, 219–228.
- SCHLUNEGGER, F. 1991: Stratigraphie, Sedimentologie und Tektonik der Unteren Süswassermolasse östlich von Thun. Unpubl. Diploma thesis Univ. Bern.
- 1995: Magnetostratigraphie und fazielle Entwicklung der Unteren Süswassermolasse zwischen Aare und Limmat. Unpubl. Ph.D. thesis Univ. Bern.
- SCHLUNEGGER, F., MATTER, A. & MANGE, M.A. 1993: Alluvial fan sedimentation and structure of the southern Molasse Basin margin, Lake Thun area, Switzerland. *Eclogae geol. Helv.* 86, 717–750.
- SCHMIDT-KITTLER, N. (ed.) 1987: International symposium on mammalian biostratigraphy and paleoecology of the European Palaeogene, Mainz, February 18th–21st 1987. *Münchner Geowiss. Abh. (A)* 10, 15–19.
- SINCLAIR, H.P. & ALLEN, P.A. 1992: Vertical versus horizontal motions in the Alpine orogenic wedge: stratigraphic response in the foreland basin. *Basin Research* 4, 215–232.
- SINCLAIR, H.D., COAKLEY, B.J., ALLEN, P.A. & WATTS, A.B. 1991: Simulation of foreland basin stratigraphy using a diffusion model of mountain belt uplift and erosion: an example from the central Alps, Switzerland. *Tectonics* 10, 599–620.
- STEININGER F.F. 1994: Proposal for the Global Stratotype Section and Point (GSSP) for the Base of the Neogene (the Palaeogene/Neogene boundary), International Commission on Stratigraphy, Subcommittee on Neogene Stratigraphy. Working Group on the Palaeogene/Neogene Boundary: Institute for Paleontology, Vienna, University of Vienna.
- STEININGER, F., BERNOR, R. & FAHLBUSCH, V. 1990: European Neogene marine/continental chronologic correlation. In: *European Neogene mammal chronology*. (Ed. by LINDSAY, E., FAHLBUSCH, V. & MEIN, P.). Plenum Press, New York, 219–228.
- STÖFFLER, D. 1977: Research drilling Nördlingen 1973: polymict breccias, crater basement, and cratering model of the Ries impact structure. *Geol. Bavarica* 75, 443–485.
- TALLING, P. & BURBANK, D.W. 1993: Assessment of uncertainties in magnetostratigraphic dating of sedimentary strata. In: *Applications of paleomagnetism to sedimentary geology*. (Ed. by AISSAOUI, D.M., MCNEILL, D.F. & HURLEY, N.F.). *Spec. Publ. Soc. econ. Paleont. Mineral.* 49, 59–70.

Manuscript received October 6, 1995

Revision accepted January 9, 1996